UNIT 8

STRESS DISTRIBUTION

Prepared by Dr. Roy E. Olson on Spring 1989

Modified by Jiunnren Lai on Fall 2003

8.1 Introduction

For many problems of practical interest, it is necessary to estimate settlements under conditions in which the induced stress varies spatially. The first steps in the analyses of such problems usually involve estimations of the initial states of stress in the soil and of the changes in these stresses during loading and as the soil again approaches equilibrium. Two methods of analysis have commonly been followed.

The first may be termed the method of *limiting equilibrium*. In this method, the stresses that would cause failure are calculated and the applied stresses are compared with the failure stresses to determine a factor of safety against complete failure. The method provides no information about deformations or states of stress within the soil mass. This method of analysis is used to determine the bearing capacity of a foundation or the stability of a slope.

In the second method of analysis, the shearing stresses in the soil are assumed to be so much less than the shearing strength that the soil can be treated as an elastic continuum and the stresses and deformations can be calculated using the theory of elasticity. This method of analysis is usually applied in the calculation of the immediate and consolidation settlements of foundations because the factor of safety of such foundations against a bearing capacity failure is usually greater than three.

The first method of analysis is reasonably accurate when the soil is in a state of incipient failure and the second method is reasonably accurate for applied stresses that are small compared with the stresses that would cause failure. In many foundation problems a certain amount of plastic deformation occurs even though the factor of safety against a total shear failure is satisfactory; thus neither approach is really correct. The finite element method of analysis is being used in attempts to solve these problems but the method has not been developed to such an extent that it can be used for routine analysis of problems in foundation engineering.

In this set of notes the assumption is made that the soil can be treated as an elastic body without excessive error, and the stresses and deformations are calculated for a variety of boundary and initial conditions. The solutions are presented in a sequence starting with the most simple idealizations for both the loading and the media and progressing toward the most complex.

In presenting the solutions it is soon discovered that just a simple tabulation of equations would require a prohibitive amount of space. As a result, no attempt is made to present all of the solutions presently available. Certain solutions, that are considered of most practical

value, are presented and papers in which the more complete solutions are published are referenced.

The theoretical solutions give total stresses in a weightless elastic medium. Total stresses are given because the soil is assumed to be a continuum. Their resolution into effective stresses and pore water pressures is a separate problem not considered in terms of the theory of elasticity.

The assumption that the medium is weightless simplifies the theoretical analyses and the form of the resulting equations. The actual state of stress is found by superimposing the stresses calculated for the weightless medium on the initial state of stress in the soil prior to application of the load.

The soil is generally assumed to be isotropic and linearly elastic so that its properties can be described using only two parameters. In most of the solutions it will be convenient to use Young's modulus, E, as one of the parameters and Poisson's ratio, n, as the other.

8.2 Notations and Definitions

The notation and sign conventions to be followed in this chapter are illustrated in Fig. 8.1 which depicts an elementary cube of soil at the origin of a Cartesian coordinate system.

A sign is given to each plane surface of the cube. A plane is positive if its outwardly directed normal points in a positive direction. Positive directions are indicated by the arrows on the axes. In Fig. 8.1, the exposed planes normal to the x and y axes are positive whereas the exposed plane normal to the z axis is negative.

Normal stresses are indicated by the symbol σ. A single subscript is used to denote the orientation of the stress. Thus, a subscript x indicates that the stress is parallel to the x axis. Compressive stresses are positive. Thus, the stress normal to a positive plane acts in the

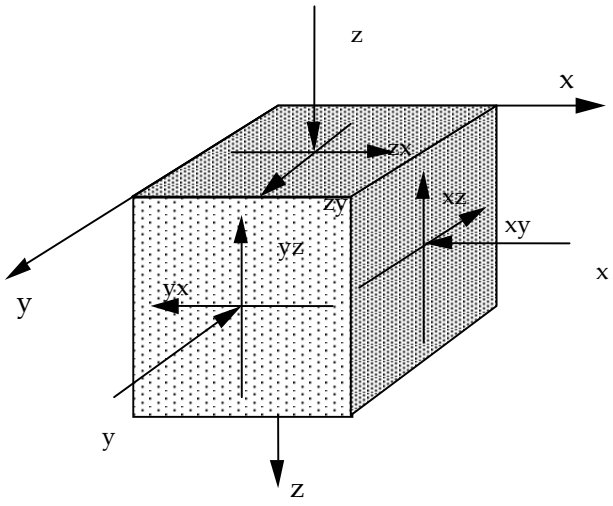

Fig. 8.1 Notation and Sign Conventions in a Cartesian Coordinate System

opposite direction of the positive, parallel axis of the coordinate system, i.e., in the negative

direction. Subscripts 1, 2, and 3 will be used to indicate the maximum, intermediate, and minor principal stresses, respectively.

Shearing stresses are denoted by the symbol τ. A dual subscript is used. The first letter of the subscript designates the plane in which the shearing stress acts by stating the axis that is normal to this plane. The second subscript designates the axis parallel to the shearing stress. Thus, τ_{xy} denotes a shearing stress parallel to the y axis in a plane perpendicular to the x axis.

A shearing stress is positive if it acts in a positive plane in a negative direction. This odd definition of the sign of a shearing stress results from the definition that compressive stresses are positive. The sign of shearing stresses will not be of interest in the text to follow so the odd definition will not cause any difficulties.

The symbols e and D will be used for linear strains and deformations, respectively. The subscript notation will be the same as used for normal stresses.

8.3 Homogeneous, Isotropic, Weightless, Linearly Elastic Half Spaces with Plane Horizontal Surfaces

8.3.1 Vertical Point Load at the Surface

The solution to the problem of calculating the stresses in an elastic half space subjected to a vertical point load at the surface will be of value in estimating the stresses induced in a deposit of soil whose depth is large compared to the dimensions of that part of the surface that is loaded. Thus, individual column footings or wheel loads may be replaced by equivalent point loads provided that the stresses are to be calculated at points sufficiently far from the point of application of the point load. The sizes of the errors involved in applying the point-load equations will be discussed subsequently.

Equations for the stresses and strains induced in a homogeneous, isotropic, weightless, linearly elastic half space, with a plane horizontal surface, by a point load perpendicular to the surface and acting at the surface, was first solved in usable form by Boussinesq (1885). The geometry of the problem is shown in Fig. 8.2.

For most practical analyses of the settlement behavior of soils, it is assumed that the volume of the soil is controlled exclusively by the vertical stress, σ_z. The vertical stress is given by:

$$\sigma_z = \frac{3P}{2\pi}\frac{z^3}{R^5} = \frac{3P}{2\pi R^2}\cos^3\beta = I\,\frac{P}{z^2} \qquad (8.1)$$

where I is termed an *influence factor.*

One of the several reasons for assuming that the soil consolidates in response to the change in vertical stress is the relative simplicity of the equations, which do not contain Poisson's ratio. The assumption is likely to be most accurate in the soil directly beneath the center of the surface load, which is the zone of most interest in settlement analyses.

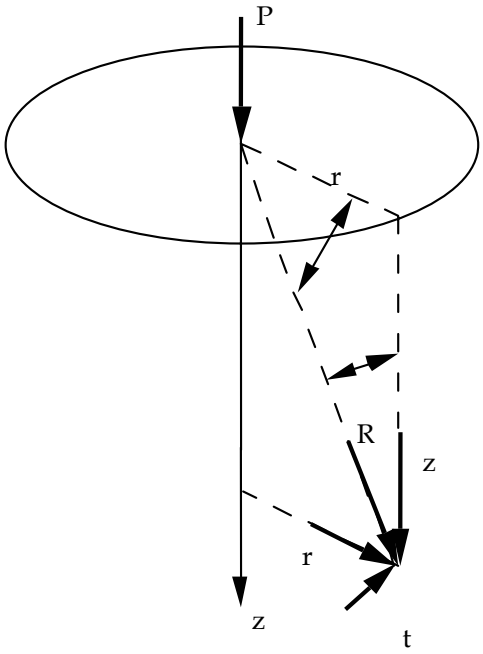

Fig. 8.2 Symbols Used in the Equations
For a Point Load Applied at the Surface

Hand calculations of the vertical normal stress are usually performed using tabulated values of the influence factor. Values for this, and other influence factors have been published by Gilboy (1933), Terzaghi (1943, pp. 481-484), Taylor (1948, p. 253), and many others. The influence factor from Eq. 8.1 is shown as a function of the ratio (r/z) in Fig. 8.3.

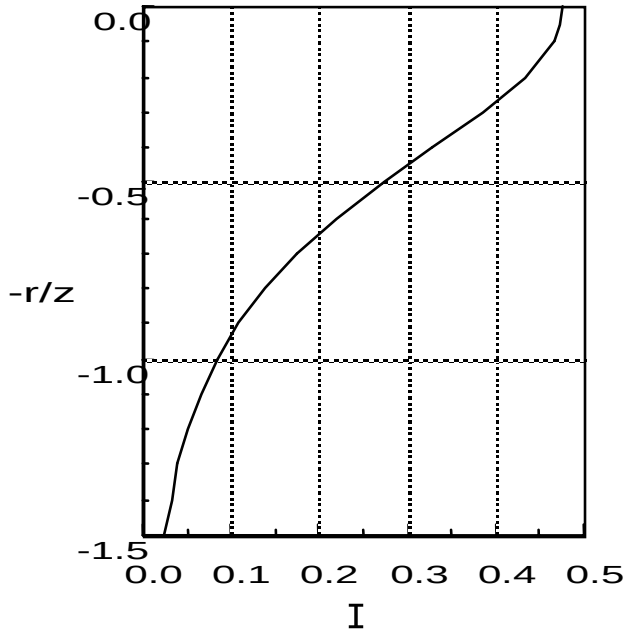

Fig. 8.3 The influence factor as a function of the ratio (r/z) from a vertical point load at the surface

The distribution of σ_z in the elastic medium is apparently radially symmetrical. The stress is infinite at the surface directly beneath the point load and decreases with the square of the depth. At any given non-zero radius, r, from the point of load application, the vertical stress is zero at the surface, increases to a maximum value at a depth where ø = 39.25 deg. (Jumikis, 1964), and then decreases with depth. At any given depth the distribution on a horizontal plane is bell shaped with the volume under the bell equal to P.

Although, for practical analyses, interest is usually restricted to the vertical normal stress, it may be of interest in some problems to estimate values for other normal stresses, and for shearing stresses. Pertinent equations follow:

$$\sigma_x = \frac{P}{2\pi}\left[3\frac{x^2z}{R^5} - (1-2\nu)\left(\frac{x^2-y^2}{Rr^2(R+z)} + \frac{y^2z}{R^3r^2}\right)\right] \tag{8.2a}$$

$$\sigma_y = \frac{P}{2\pi}\left(3\frac{y^2z}{R^5} - (1-2\nu)\frac{y^2-x^2}{Rr^2(R+z)} + \frac{x^2z}{R^3r^2}\right) \tag{8.2b}$$

$$\sigma_r = \frac{P}{2\pi}\left[3\frac{r^2z}{R^5} - (1-2\nu)\frac{R-z}{Rr^2}\right] \tag{8.2c}$$

$$\sigma_t = \frac{P}{2\pi}\left[(1-2\nu)\left(\frac{1}{r^2} - \frac{z}{R^3} - \frac{z}{Rr^2}\right)\right] \tag{8.2d}$$

$$\tau_{rz} = \frac{3P}{2\pi}\frac{rz^2}{R^5} \tag{8.2e}$$

$$\tau_{zx} = \frac{3P}{2\pi}\frac{z^2x}{R^5} \tag{8.2f}$$

$$\tau_{zy} = \frac{3P}{2\pi}\frac{z^2y}{R^5} \tag{8.2g}$$

$$\tau_{rt} = \tau_{tr} = 0 \tag{8.2h}$$

Influence diagrams could be presented to show the spatial distribution of these normal and shearing stresses but the large number of equations, the fact that some of the stresses vary with Poisson's ratio, and the limited practical interest, suggest that it will be more efficient to apply the equations directly whenever the need arises.

Occasionally it may be of interest to estimate the induced principal stresses in a weightless medium. If three orthogonal sets of normal and shearing stresses are known, associated with some cartesian coordinate system x-y-z, then the principal stresses are the three roots of the equation:

$$\sigma^3 - I_1\sigma^2 + I_2\sigma - I_3 = 0 \tag{8.3a}$$

where:

$$I_1 = \sigma_x + \sigma_y + \sigma_z \tag{8.3b}$$

$$I_2 = \sigma_x\sigma_y + \sigma_y\sigma_z + \sigma_z\sigma_x - \tau_{xy}^2 - \tau_{yz}^2 - \tau_{zx}^2 \tag{8.3c}$$

$$I_3 = \sigma_x\sigma_y\sigma_z + 2\tau_{xy}\tau_{yz}\tau_{zx} - \sigma_x\tau_{yz}^2 - \sigma_y\tau_{xz}^2 - \sigma_z\tau_{xy}^2 \tag{8.3d}$$

For the particular case of the point load, all planes containing the line of action of the point load, i.e., all vertical planes through the point load, are principal planes by reason of symmetry. Thus, the r-t-z coordinate system is used and one of the principal stresses is given by Eq. 2d. The other two principal stresses are the roots of:

$$\sigma = \frac{1}{2}\left[(\sigma_z - \sigma_r) \pm \sqrt{(\sigma_z - \sigma_r)^2 + (2\tau_{rz})^2}\right] \tag{8.4}$$

In the special case that Poisson's ratio is 0.5 the equations for the principal stresses reduce to the following simple forms:

$$\sigma_1\ (\nu=0.5) = \frac{3P}{2\pi}\frac{z}{R^3} \tag{8.5a}$$

$$\sigma_2\ (\nu=0.5) = \sigma_3\ (\nu=0.5) = 0 \tag{8.5b}$$

The maximum principal stress is directed along the radius vector R.

It must be emphasized that the calculated principal stresses are for a weightless medium. In real media the stresses produced by a concentrated load are superimposed on an existing stress field so that the real principal stresses will have neither the values nor the orientations that have been calculated. Actual principal stresses can be estimated by inserting the sums of the initial and induced stresses into Eq. 8.3a and then finding the roots.

The deformations are given by the following equations:

$$\Delta_z = \frac{P}{2\pi}\frac{1+\nu}{E}\left[\frac{z^2}{R^3} + (1-\nu)\frac{2}{R}\right] \tag{8.6a}$$

$$\Delta_x = \frac{P}{2\pi}\frac{1+\nu}{E}\left[\frac{xz}{R^3} - (1-2\nu)\frac{x}{R(R+z)}\right] \tag{8.6b}$$

$$\Delta_y = \frac{P}{2\pi}\frac{1+\nu}{E}\left[\frac{yz}{R^3} + (1-2\nu)\frac{y}{R(R+z)}\right] \tag{8.6c}$$

$$\Delta_r = \frac{P}{2\pi}\frac{1+\nu}{E}\left[\frac{rz}{R^3} + (1-2\nu)\frac{r}{R(R+z)}\right] \tag{8.6d}$$

Because of symmetry, the tangential deformation is zero.
Most of the equations for stresses and deformations induced by a vertical point load were presented because solutions for many other loadings have been obtained by integration of the

equations for point loads. For practical work the equations of most interest are for the vertical stress, the vertical deformation, and perhaps for the maximum shearing stress. Occasionally the equations for the principal stresses are of interest. For most of the loadings, solutions will be presented for only these parameters.

8.3.2 Vertical point load applied within the medium

For most practical problems in foundation engineering the load is applied at some depth within the soil, not at the surface. In attempting to estimate the induced state of stress in the soil it may be of interest to be able to calculate the stresses induced in an elastic half space by a point load applied at some finite depth. This problem was solved by Mindlin (1936). The geometry of the problem is shown in Fig. 8.4. The following equations give the pertinent stresses and deformations:

$$\sigma_z = \frac{P}{8\pi(1-\nu)}\left[F_1 - F_2 + F_3 + F_4 + F_5\right] \tag{8.7a}$$

where

$$F_1 = \frac{(1-2\nu)(z-c)}{R_1^3} \tag{8.7b}$$

$$F_2 = \frac{(1-2\nu)(z-c)}{R_2^3} \tag{8.7c}$$

$$F_3 = \frac{3(z-c)^3}{R_1^5} \tag{8.7d}$$

$$F_4 = \frac{3(3-4\nu)(z)(z+c)^2-3c(z-c)(5z-c)}{R_2^5} \tag{8.7e}$$

$$F_5 = \frac{30cz(z+c)^3}{R_2^7} \tag{8.7f}$$

$$\tau_{rz} = \frac{Pr}{8\pi(1-\nu)}\left[\frac{1-2\nu}{R_1^3} - \frac{1-2\nu}{R_2^3} + \frac{3(z-c)^2}{R_1^5} - \frac{3(3-4\nu)(z)(z+c)-3c(3z+c)}{R_2^5} - \frac{30cz(z+c)^2}{R_2^7}\right] \tag{8.7g}$$

$$\Delta_z = \frac{P}{16\pi G(1-\nu)}\left[\frac{(3-4\nu)}{R_1} + \frac{8(1-\nu)^2-(3-4\nu)}{R_2} + \frac{(z-c)^2}{R_1^3} + \frac{(3-4\nu)(z+c)^2-2cz}{R_2^3} + \frac{6cz(z+c)^2}{R_2^5}\right] \tag{8.7h}$$

Equations for other stresses and deformations will be found in Mindlin (1936).

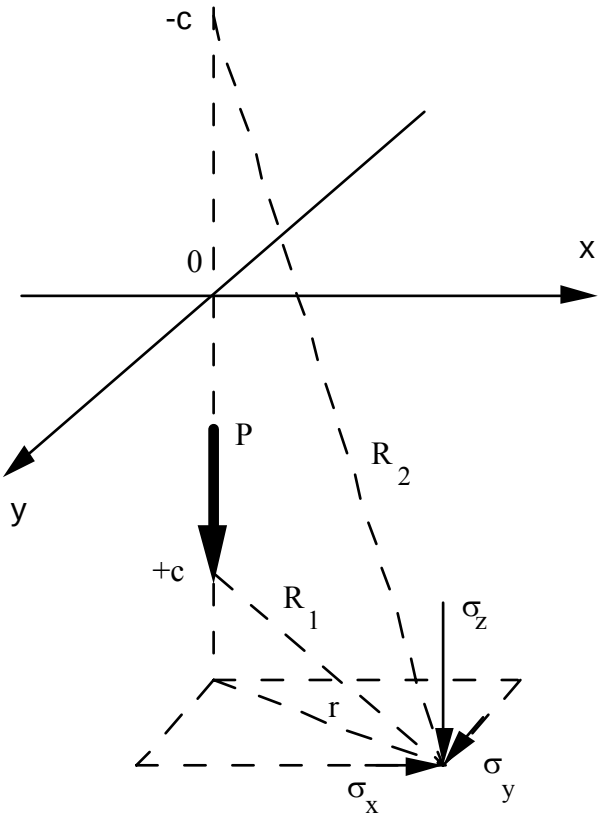

Fig. 8.4 Geometry of the Problem Solved by Mindlin

According to Eq. 8.7a the vertical normal stress is a tensile stress for the part of the medium with r/c less than about 0.6 and z ranging from 0 to c. In the case of a real soil, these induced tensile stresses are superimposed on top of compressive stresses so that the resulting total stress may be compressive throughout much of this zone provided that the concentrated load is of small magnitude or buried deeply. The zone immediately above the point load will always be subjected to an absolute tensile stress, however, and the zone just below the point load to an infinite compressive stress. St. Venant's principle is applied and Mindlin's equations are used to calculate stresses and deformations at points sufficiently far removed from the point of application of the load so that the difference between the stresses induced by the real loading over a small area and the stresses theoretically induced by a point load do not differ materially. St. Venant's principle will be discussed further subsequently.

The tensile stresses in the elastic medium above the point of application of the load cause the vertical normal stresses to be more widely distributed than they would be if the point load had been applied at the surface. Accordingly, the vertical normal stresses in the medium at finite non-zero distances directly beneath the point load must be smaller when the point load is buried than when it is at the surface. Such a comparison is shown in Fig. 8.5 where an influence factor equal to $\sigma_Z\ c^2/P$ is plotted versus r/c for a plane at a depth of 0.5c beneath a vertical point load. The influence of the medium between depths of 0 and c on the stresses at greater depth is taken into account with the Mindlin solutions but not in the Boussinesq solution.

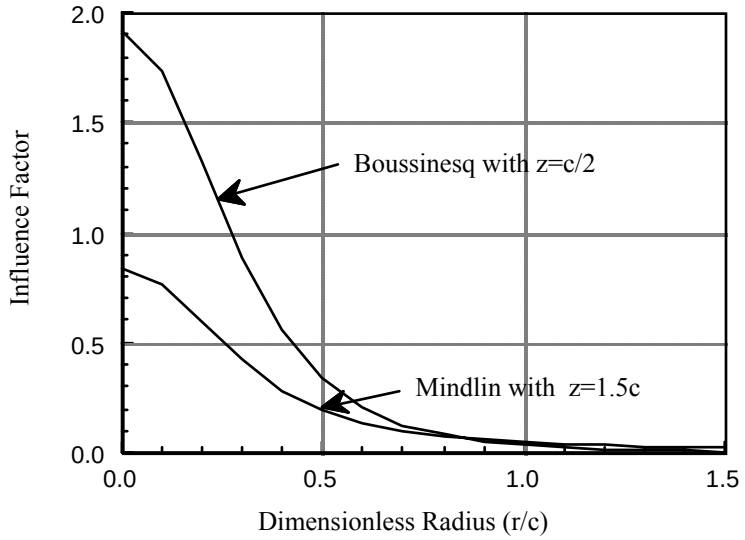

Fig. 8.5 Comparison of Influence Factors for the Vertical Compressive Stress at a Depth of 0.5c Below a Vertical Point Load, for the Point Load at the Surface (Boussinesq) or Buried at a Depth c (Mindlin).

For the Boussinesq case the point load is at the Surface; for the Mindlin case the point load is at a depth c and Poisson's Ratio is 0.333. In both cases, the stresses are computed at a depth 0.5c below the point load.

As the depth of burial of the point load increases, the induced stresses approach those for a point load buried in an infinite medium. The solution for the state of stress in an indefinitely extended, weightless, homogeneous, isotropic, linearly elastic medium was first obtained by Kelvin in 1848 and have been reported by Timoshenko and Goodier (1951, pp. 354-356) and others.

8.3.3 Horizontal point load at the surface

According to Todhunter and Pearson (1893, Part II), solutions for the stresses and deformations in a semi-infinite, homogeneous, isotropic, weightless, linearly elastic medium with a plane, horizontal surface, acted upon by a horizontal point load applied in the surface, were first obtained by Cerruti (1882) and Boussinesq (1885). More recently, various of the solutions have been reported by Vogt (1925), Westergaard (1940), Mindlin (1936), and Holl (1941). The equation for the vertical stress is:

$$\sigma_z = \frac{3S}{2\pi}\frac{xz^2}{R^5} \tag{8.8}$$

where S is the applied force and the other symbols are as defined in Fig. 2. Equations for other stresses will be found in the afore mentioned references.

It is interesting to note that the vertical normal stress is again independent of Poisson's ratio. Calculations show that the vertical normal stress directly beneath the point of application of the horizontal force are considerably smaller than those induced by a vertical force of the same magnitude so that the horizontal component of surface forces are often ignored in

calculating the vertical normal stresses.

8.3.4 Oblique point loads at the surface

Because of the assumption that the medium is linearly elastic, the stresses induced by oblique point loads at the surface are obtained simply by adding the stresses calculated for the vertical and horizontal components of the oblique force.

8.3.5 Horizontal point loads applied within the medium

Equations for the stresses and deformations induced by forces applied within the elastic medium parallel to the surface, have been presented by Mindlin (1936).

8.3.6 Vertical line load at the surface

Equations for the stresses and deformations induced in an elastic half space by a line load of infinite length acting normal to the plane surface can be developed by integrating Boussinesq's solutions for the point load. Solutions attributed to Mitchell (1899) and Melan (1919, 1932) have been presented by Timoshenko (1934), Gray (1936, Newmark (1940), Holl (1941), and others. The geometry of the problem is shown in Fig. 8.6.

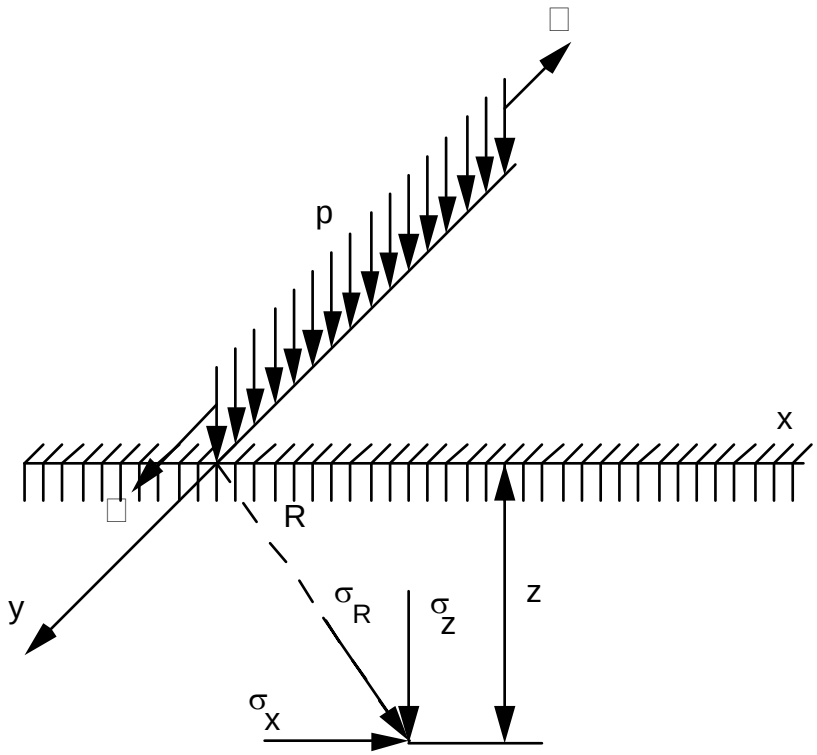

Fig. 8.6 Geometry of the Problem Involving a Uniform Line Load of Infinite Surface at the Surface

The pertinent normal stresses are given by the following equations:

$$\sigma_x = \frac{2p}{\pi}\frac{x^2 z}{R^4} \tag{8.9a}$$

$$\sigma_y = \sigma_2 = \frac{2p\nu}{\pi}\frac{z}{R^2} \tag{8.9b}$$

$$\sigma_z = \frac{2p}{\pi}\frac{z^3}{R^4} \tag{8.9c}$$

$$\sigma_R = \sigma_1 = \frac{2p}{\pi}\frac{z}{R^2} \tag{8.9d}$$

$$\sigma_t = \sigma_3 = 0 \tag{8.9e}$$

Again, the stress of greatest practical interest is probably σ_z. Because the stresses from the infinite line load are effectively distributed in only one horizontal direction, as opposed to two for the point load, the vertical normal stresses beneath the line of application of the load decrease only with the first power of the depth, and at any give depth are distributed more widely than for the point load, the vertical normal stress does not depend on Poisson's ratio.

The applied principal stresses are easily calculated in the problem. The maximum principal stress acts along the radius vector R. As for all subsequent plane strain problems, the intermediate principal stress acts parallel to the y axis.

Because of symmetry, the shearing stress in all planes normal to the y axis must be zero. The orthogonal shearing stress is:

$$\tau_{xz} = \frac{2p}{\pi}\frac{xz^2}{R^4} \tag{8.10a}$$

The maximum shearing stress at any point is:

$$\tau_{max} = \frac{p}{\pi}\frac{z}{R^2} \tag{8.10b}$$

The foregoing equations are of value in estimating the response of a soil to a surface loading by a long narrow footing. The equations are somewhat simpler to use than those to be developed subsequently for rectangular strip loads but, of course, cannot be applied in the immediate vicinity of the strip footing.

For some settlement analyses it is of interest to calculate the change in vertical normal stress caused by a line load of finite length. Fadum (1948) integrated Boussinesq's solution for a surface point load to obtain the following equation for the vertical stress at a depth z under one end of the line load:

$$\sigma_z = \frac{p}{2\pi} \frac{Lz^3}{x^2+z^2} \frac{1}{\sqrt{x^2+z^2+L^2}} \left[\frac{1}{x^2+z^2+L^2} + \frac{2}{x^2+z^2} \right] \quad (8.11)$$

The coordinate system is the same as that used for the infinitely long line load. The stress is calculated at the point x,O,z for a line load extending from 0,0,0 to 0,L,0. Stresses at other points are calculated according to the principle of superposition. Thus, if the vertical stress in a plane at a distance y' beyond the end of a line element of length L is to be calculated, the following equation would be applied:

$$\sigma_z(L) = \sigma_z(L+y') - \sigma_z(y') \quad (8.12)$$

where the symbols $\sigma_z(L)$, $\sigma_z(L+y')$, and $\sigma_z(y')$ indicate the vertical stresses at a depth z and coordinate x, calculated using Fadum's equation for line elements of lengths L, L+y' and y' respectively.

8.3.7 Horizontal line load at the surface

Cerruti's solutions for stresses induced by a point shearing force applied at the surface were integrated by Holl (1941) to obtain solutions for the stresses induced by horizontal line loads applied at the surface.

8.3.8 Horizontal and vertical line loads within the medium

Equations for the stresses induced in an elastic medium by line loads applied within the medium have been presented by Melan (1932).

8.3.9 Vertical stress covering half the surface

Equations have been developed to give the stresses and deflections caused by vertical loads distributed across the area defined by $0<x<\infty$, $-\infty<y<+\infty$, and $z = 0$, i.e., covering half the surface. For purposes of settlement analyses, these equations are mainly of use for estimating the states of stress near the edges of wide fills. Unfortunately, these are precisely the zones where the shearing stresses are likely to be so high that the assumption of linear elasticity for the soil is unacceptable. In any case, the equations were obtained by simply integrating the Boussinesq solutions for point loads and thus do not take into account the influence of the flexural properties of the fill on stress distribution. The equations for both stresses and deformations were developed by Carothers (1920, 1924) and have been tabulated for ready reference by Gray (1936) and Holl (1941).

8.3.10 Strip loadings

The term *strip loading* will be used to indicate a loading that has a finite width along the x axis but an infinite length along the y axis. Solutions have been obtained by Carothers (1920) for a variety of distributions of stress across the width of the strip. In this section, only the equations pertaining to a uniform load and a semi-embankment load will be considered. Equations for other distributions of load will be found in Gray (1936) and Holl (1941). The solutions do not take into account the flexural properties of the embankments.

Uniformly loaded strip. The geometry of the problem is shown in Fig. 8.7. The loading is intended as a first approximation of the loading applied by a long wall footing. The following

equations give the normal stresses in the directions of the coordinate axes:

$$\sigma_x = \frac{p}{\pi} (\alpha - \sin \alpha \cos 2\beta) \quad (8.13a)$$

$$\sigma_y = \frac{2p\nu}{\pi} \alpha \quad (8.13b)$$

$$\sigma_z = \frac{p}{\pi} (\alpha + \sin \alpha \cos 2\beta) \quad (8.13c)$$

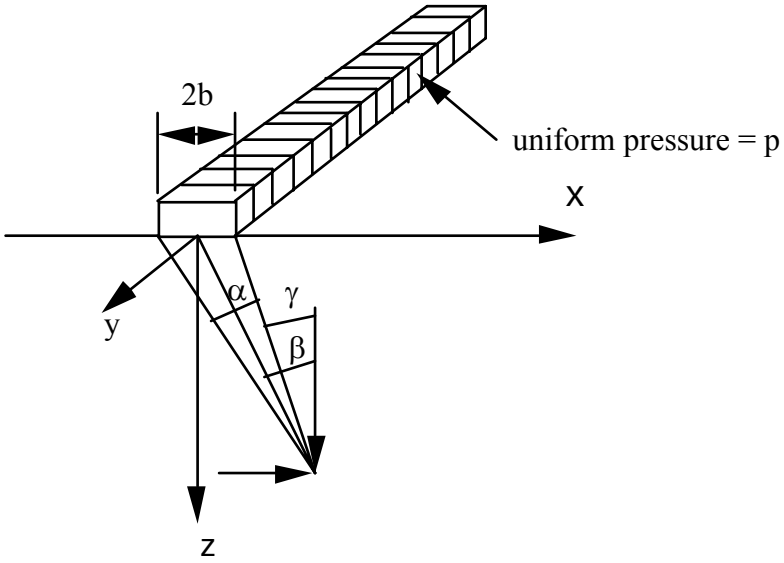

Fig. 8.7 Geometry of the Problem Involving a Uniform Strip Load of Infinite Length at the Surface

Influence factors for the stresses in the x and z directions have been presented by Jurgenson (1934) and those for the y direction are easily calculated. Influence factors for the vertical stress are plotted in Fig. 8.8.

The shearing stresses are:

$$\tau_{xz} = \frac{p}{\pi} \sin \alpha \sin 2\beta \quad (8.14a)$$

$$\tau_{max} = \frac{p}{\pi} \sin \alpha \quad (8.14b)$$

The principal stresses are:

$$\sigma_1 = \frac{p}{\pi} (\alpha + \sin \alpha) \quad (8.15a)$$

$$\sigma_3 = \frac{p}{\pi} (\alpha - \sin \alpha) \quad (8.15b)$$

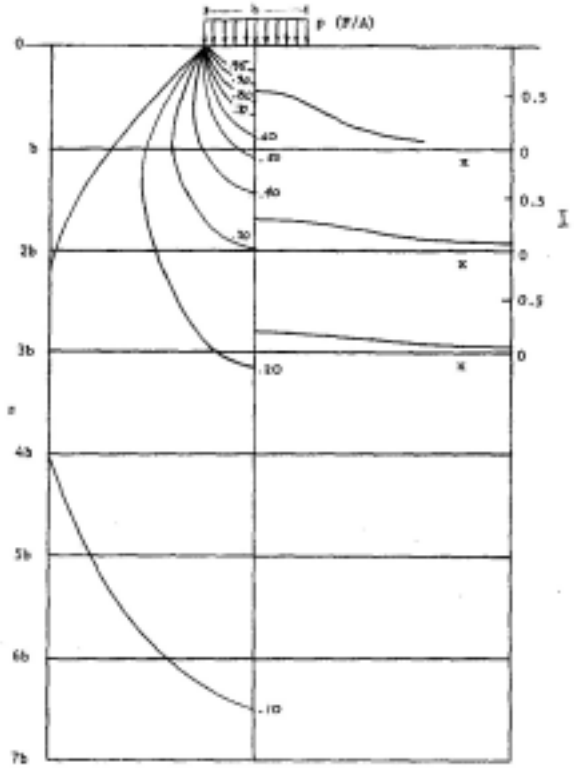

Fig. 8.8 Influence factors for the vertical compressive stress beneath a uniformly loaded, infinitely long, strip.

The intermediate principal stress is σ_y.

Equations for the strains in the vertical direction (Gray, 1936) can be integrated for finite depths of subsoil to obtain estimates of deformations.

Semi-embankment. The geometry of this problem is shown in Fig. 8.9.

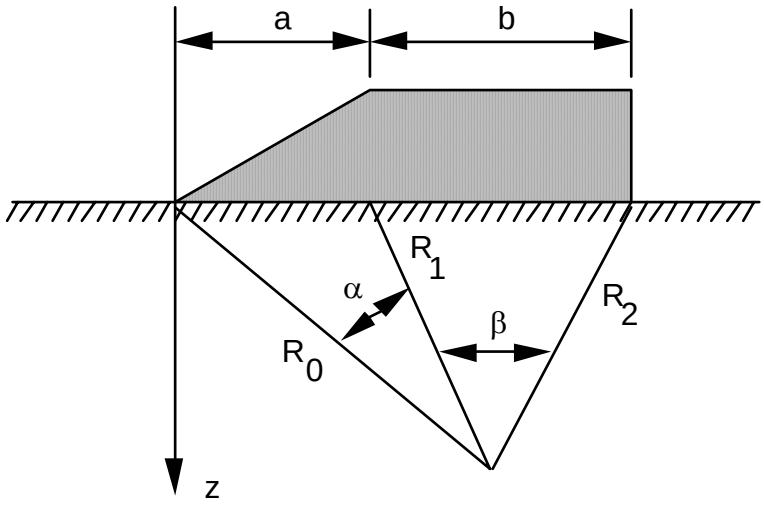

Fig. 8.9 Geometry Involved in the Equations for a Semi-Embankment Loading

The loading simulates part of an embankment with one sloping edge and one edge bounded by a vertical plane. Equations have been derived for the more general case of unsymmetrical embankments with sloping edges by Carothers (1920) but are too long to be repeated here. For the semi-embankment the stresses in the directions of the three Cartesian coordinate axes are:

$$\sigma_x = \frac{p}{\pi a}\left[a\beta + x\alpha + \frac{az}{R_2^2}(x-a-b) + 2z\ln\left(\frac{R_1}{R_2}\right)\right] \tag{8.16a}$$

$$\sigma_y = \frac{2p\nu}{\pi a}\left[a\beta + x\alpha + z\ln\left(\frac{R_1}{R_2}\right)\right] \tag{8.16b}$$

$$\sigma_z = \frac{p}{\pi a}\left[a\beta + x\alpha - \frac{az}{R_2^2}(x-a-b)\right] \tag{8.16c}$$

The influence diagram for the vertical stress at any depth z directly beneath the vertical edge of the semi-embankment (Osterberg, 1957) is shown in Fig. 8.10. If the induced vertical

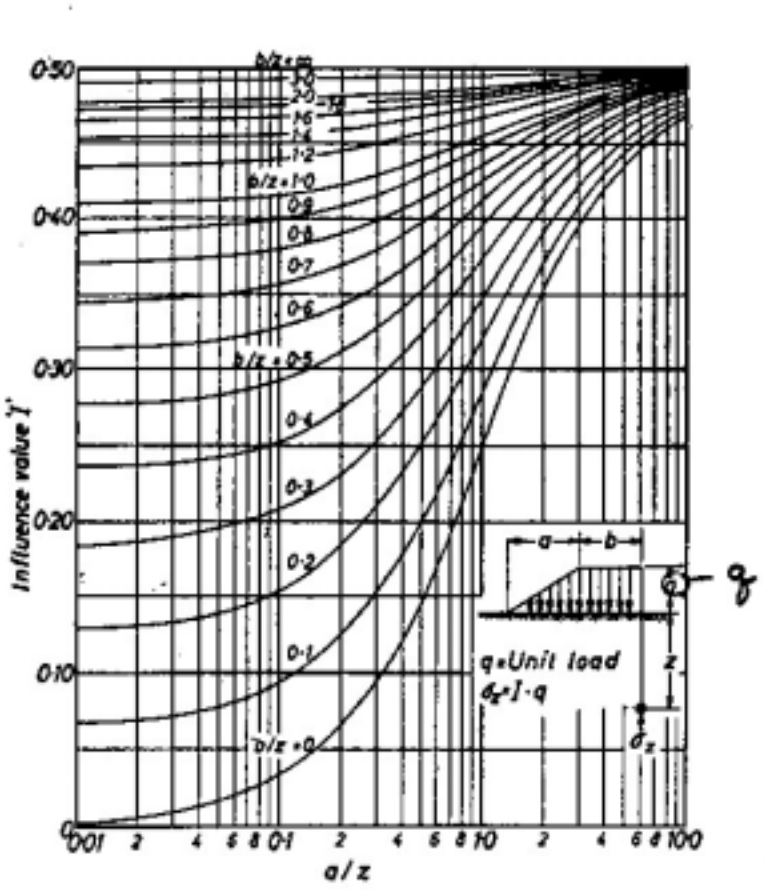

Fig. 8.10 Osterberg's Influence Chart for a Semi-Embankment Loading

stress is to be estimated beneath the central part of an embankment, then the embankment

loading diagram is split by a vertical plane, parallel to the axis of the embankment, and passing through the point where the stress is to be estimated. The plane cuts the embankment into two semi-embankments. The stresses are calculated for the two semi-embankments separately and are added to obtain the total stress. Stresses at other locations are obtained by suitable additions and subtractions of surface loadings.

Equations for the principal stresses, shearing stresses, and strains have been summarized by Gray (1936).

8.3.11 Loading of circular areas at the Surface

Equations for stresses and deformations in a half space induced by loads applied over circular areas at the surface are often used when the load is applied by circular storage tanks with flexible bases, by circular or octagonal footings or by tires. The first solutions (Carothers, 1924; Love, 1929) were not in forms that could be used in engineering practice. Foster and Ahlvin (1954) and Ahlvin and Ulery (1962) solved Love's equations and presented influence diagrams and tables of coefficients, respectively, that allow the stresses and deformations to be calculated using simple equations together with the coefficients from the graphs or tables. For use in foundation engineering, the induced vertical stress would appear to be of main interest. The variation of the induced vertical stress with respect to radius and depth, for a uniform load applied over the circular area, is shown in Fig. 11. The stresses for non-uniform applied loads that are symmetrical about the axis of the circular area may be calculated by applying the principal of superposition. As for the strip loadings, the equations ignore the flexural properties of the foundation and thus apply only to a perfectly flexible, frictionless foundation subjected to the assumed distribution of stress.

For the special case of calculating the vertical compressive stress at some depth directly beneath the centerline of a circular area subjected to a radially symmetrical distribution of stress, it is a simple matter to integrate Boussinesq's equations for point loading to obtain a solution. Solutions for various distributions of stress have been obtained by Foppl (Cummings, 1936), Cummings (1936), Krynine (1936) and Harr and Lovell (1963, from Egorov, 1958) . For the case of a uniform surface pressure, the vertical compressive stress at a depth z beneath the center line is:

$$\sigma_z = p\left[1 - \left(\frac{1}{1 + \left(\frac{R}{z}\right)^2}\right)^{3/2}\right] \qquad (8.17)$$

where R is the radius of the loaded area.

Kezdi (1957) presented an equation for σ_z under the centerline of a uniformly loaded circular area at a depth z and plotted σ_z/p versus z/R for values of z/R ranging from 0 to infinity.

The equations for the vertical deformation of the surface are of particular interest because field plate loading tests are usually performed using circular plates. If the deformation is measured in the field, the equations can be solved for a term which contains only the elastic coefficients and which may be used in calculating the initial settlements of foundations in that soil. The surface settlement for the case of a uniform pressure, p, applied over a circular area of radius R, is (Boussinesq, 1885, p. 140):

$$\Delta_z = p\,R\,\frac{2(1-\nu^2)}{E}\,I \tag{8.18}$$

The influence factor equals 1.00 beneath the center of the plate and 0.637 beneath the edge. Other values may be obtained from the solutions of Ahlvinand Ulery (1962), the influence diagrams of Newmark (1947), equations by Schiffman (1963), or by direct solution of the pertinent equations. For a saturated soil, Poisson's ratio may be assumed to equal to 0.5 and Young's modulus may be calculated.

For a rigid circular plate, the deformation is (Newmark, 1940):

$$\Delta_z = \frac{P}{2R}\,\frac{(1-\nu^2)}{E} \tag{8.19}$$

where P is the total vertical force applied to the plate. The distribution of stress across the base of the rigid plate was given by Boussinesq (Timoshenko and Goodier, 1951) as:

$$p = \frac{P}{2\pi R\sqrt{R^2-r^2}} \tag{8.20}$$

where p is the contact pressure and r is the variable radial distance. Apparently, the contact stress varies from half the average pressure at the centerline to infinity under the edge.

8.3.12 Uniformly loaded rectangular area at the surface

The stresses and deformations generated in an elastic half space by a uniform, normal, surface pressure applied over a rectangular area, can be found by subdividing the rectangular area into sufficiently small blocks and treating the stress applied by each block as a point load. Theoretically exact solutions may be obtained by integration. Newmark (1935) performed the integration and gave the following equation for the vertical normal stress beneath a corner of the rectangular area:

$$\frac{\sigma_z}{p} = \frac{1}{4\pi}\left[F\left(1+\frac{z^2}{R^2}\right) + \sin^{-1}F\right] \tag{8.21a}$$

where:

$$F = \frac{2ABzR}{z^2R^2+A^2B^2} \tag{8.21b}$$

$$R = \sqrt{A^2 + B^2 + z^2} \tag{8.21c}$$

where p is the uniform vertical pressure applied over a rectangular area of dimensions A by B on a horizontal plane surface, and z is the depth beneath one corner to the point at which the vertical normal stress is to be calculated. The entire right side of Eq. 8.21a can be considered an influence factor dependent on two dimensionless factors: m = A/z and n = B/z. Since A and B can be interchanged in Eq. 8.21a without changing the stress, it is apparent that m and

n are also interchangeable. Values for the influence factor were calculated by Newmark (1935) and have been presented in tabular or graphical form by Fadum (1948), Spangler (1951), Taylor (1948), and others. Because of their usefulness, the influence factors have been tabulated in Table 8.1 and presented graphically in Fig. 8.12.

Table 8.1. Influence Factors for the Vertical Compressive Stress Beneath One Corner of a Uniformly Loaded RectangularArea at the Surface

m/n	0.1	0.2	0.3	0.4	0.5	0.6	0.7	0.8	0.9
0.1	0.005	0.009	0.013	0.017	0.020	0.022	0.024	0.026	0.027
0.2	0.009	0.018	0.026	0.033	0.039	0.043	0.047	0.050	0.053
0.3	0.013	0.026	0.037	0.047	0.056	0.063	0.069	0.073	0.077
0.4	0.017	0.033	0.047	0.060	0.071	0.080	0.087	0.093	0.098
0.5	0.020	0.039	0.056	0.071	0.084	0.095	0.103	0.110	0.116
0.6	0.022	0.043	0.063	0.080	0.095	0.107	0.117	0.125	0.131
0.7	0.024	0.047	0.069	0.087	0.103	0.117	0.128	0.137	0.144
0.8	0.026	0.050	0.073	0.093	0.110	0.125	0.137	0.146	0.154
0.9	0.027	0.053	0.077	0.098	0.116	0.131	0.144	0.151	0.162
1.0	0.028	0.055	0.079	0.101	0.120	0.136	0.149	0.160	0.168
1.2	0.029	0.057	0.083	0.106	0.126	0.143	0.157	0.168	0.178
1.5	0.030	0.059	0.086	0.110	0.131	0.149	0.164	0.176	0.186
2.0	0.031	0.061	0.089	0.113	0.135	0.153	0.169	0.181	0.192
2.5	0.031	0.062	0.090	0.115	0.137	0.155	0.170	0.183	0.194
3.0	0.032	0.062	0.090	0.115	0.137	0.156	0.171	0.184	0.195
5.0	0.032	0.062	0.090	0.115	0.137	0.156	0,172	0.185	0.196
10.0	0.032	0.062	0.090	0.115	0.137	0.156	0.172	0.185	0.196
∞	0.032	0.062	0.090	0.115	0.137	0.156	0.172	0.185	0.196

m/n	1.0	1.2	1.5	2.0	2.5	3.0	5.0	10.0	∞
0. 1	0.028	0.029	0.030	0.031	0.031	0.032	0.032	0.032	0.032
0.2	0.055	0.057	0.059	0.061	0.062	0.062	0.062	0.062	0.062
0.3	0.079	0.083	0.086	0.089	0.090	0.090	0.090	0.090	0.090
0.4	0.101	0.106	0.110	0.113	0.115	0.115	0.115	0.ll5	0.115
0.5	0.120	0.126	0.131	0.135	0.137	0.137	0.137	0.137	0.137
0.6	0.136	0.143	0.149	0.153	0.155	0.156	0.156	0.156	0.156
0.7	0.149	0.157	0.164	0.169	0.170	0.171	0.172	0.172	0.172
0.8	0.160	0.168	0.176	0.181	0.183	0.184	0.185	0.185	0.185
0.9	0.168	0.178	0.186	0.192	0.194	0.195	0.196	0.196	0.196
1.0	0.175	0.185	0.193	0.200	0.202	0.203	0.204	0.205	0.205
1.2	0.185	0.196	0.205	0.212	0.215	0.216	0.217	0.218	0.218
1.5	0.193	0.205	0.215	0.223	0.226	0.228	0.229	0.230	0.230
2.0	0.200	0.212	0.223	0.232	0.236	0.238	0.239	0.240	0.240
2.5	0.202	0.215	0.226	0.236	0.240	0.242	0.244	0.244	0.244
3.0	0.203	0.216	0.228	0.238	0.242	0.244	0.246	0.247	0.247
5.0	0.204	0.217	0.229	0.239	0.244	0.246	0.249	0.249	0.249
10.0	0.205	0.218	0.230	0.240	0.244	0.247	0.249	0.250	0.250
∞	0.205	0.218	0.230	0.240	0.244	0.247	0.249	0.250	0.250

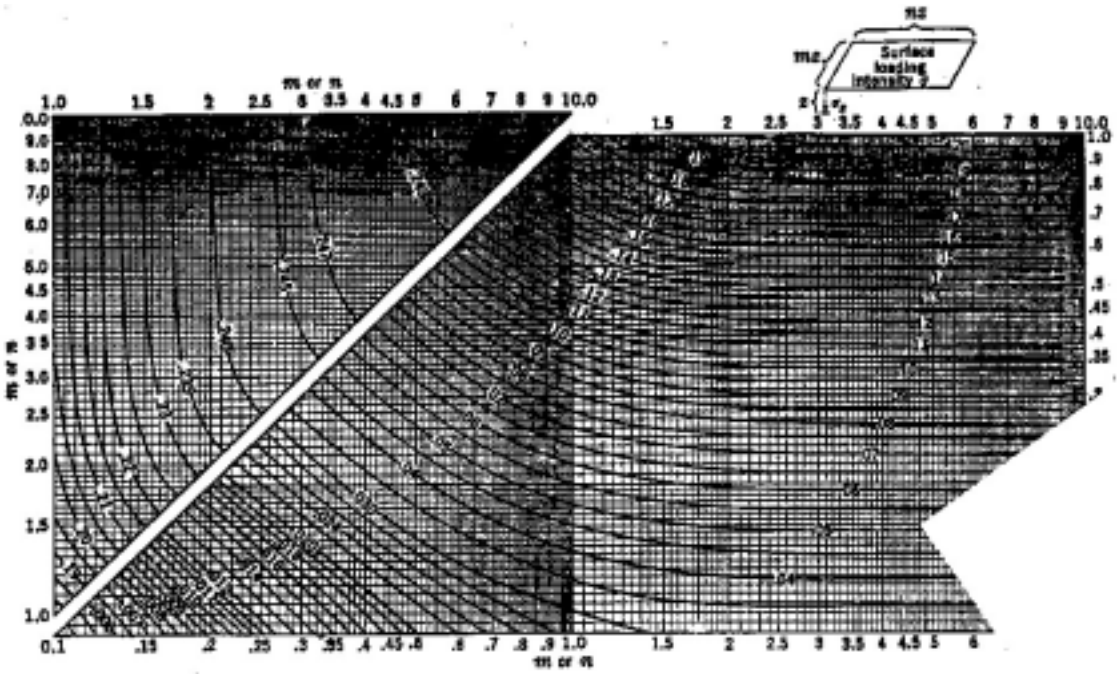

Fig. 8.12 Influence Diagram for the Vertical Compressive Stress Beneath One Corner of a Uniformly Loaded Rectangular Area at the Surface

The vertical normal stress induced at any depth by the stress on a rectangular area located any place on the surface can be found by suitable addition and or subtraction of the stresses obtained using the foregoing solutions. For example, the stress at point A in Fig. 8.13 caused by the stress applied over the area abcd, designated as σ_z(abcd) is:

$$\sigma_z(abcd) = \sigma_z(ofcg) - \sigma_z(ofbh) - \sigma_z(oedg) + \sigma_z(oeah)$$

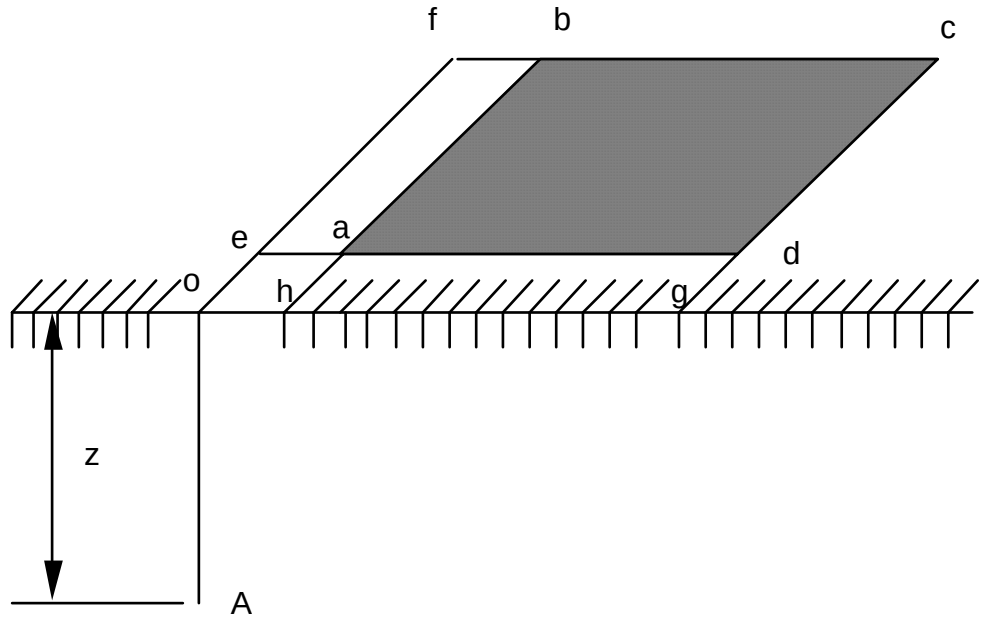

Fig. 8.13 Method of Calculating the Vertical Compressive Stress at Point A Caused by a Uniform Stress Applied to an Area abcd

Table 8.2 Boussinesq Influence Values for the Vertical Compressive Stress Beneath the Center of Footings

Depth-Width Ratio	Round	Rectangular with L/W Ratios as Shown					
	1	1	1.25	1.5	2.0	5	∞
0.02	100	100	100	100	100	100	100
0.04	100	100	100	100	100	100	100
0.06	100	100	100	100	100	100	100
0.08	100	100	100	100	100	100	100
0.10	99	99	99	99	99	100	100
0.12	99	99	99	99	99	99	99
0.14	98	98	98	98	99	99	99
0.16	97	98	98	98	99	99	99
0.18	96	97	98	98	98	98	98
0.20	95	96	97	97	97	98	98
0.22	94	95	96	96	97	97	97
0.24	92	94	95	95	96	96	97
0.26	90	92	94	94	95	96	96
0.28	88	91	93	93	94	94	95
0.30	86	89	91	92	93	94	94
0.32	84	87	90	91	92	93	93
0.34	82	85	88	90	91	91	92
0.36	80	84	86	88	90	90	91
0.38	77	82	85	87	88	89	89
0.40	75	80	83	85	87	88	88
0.42	73	78	81	84	86	87	87
0.44	71	76	80	82	84	85	86
0.46	69	74	78	80	83	84	85
0.48	66	72	76	79	81	83	84
0.50	64	70	74	77	80	82	83

Depth-Width Ratio	Round	Rectangular with L/W Ratios as Shown					
	1	1	1.25	1.5	2.0	5	∞
0.52	62	68	73	76	79	80	81
0.54	60	66	71	74	77	79	80
0.56	58	64	69	72	76	78	78
0.58	56	62	68	71	74	77	77
0.60	54	61	66	69	73	75	76
0. 62	52	59	64	68	71	74	75
0.64	50	57	63	66	70	72	73
0.66	49	55	61	65	68	71	72
0.68	48	54	59	63	67	70	71
0.70	46	52	58	62	66	69	70
0.92	33	38	43	47	52	56	59
0.94	32	37	42	46	51	56	58
0.96	31	36	41	45	50	55	57
0.98	30	35	40	44	49	55	56
1.00	29	34	39	43	48	54	55
1.02	28	33	38	42	48	53	54
1.04	27	32	37	40	46	52	53
1.06	26	31	36	39	45	52	53
1.08	25	30	35	39	44	51	52
1.10	25	29	34	38	43	50	51
1.12	24	28	33	37	42	50	50
1.14	23	28	32	36	41	49	50
1.16	23	27	32	35	40	48	49
1.18	22	26	31	34	40	48	48
1.20	21	25	30	34	39	47	48
1.22	21	25	30	33	38	46	47
1.24	20	24	29	32	38	46	46
1.26	20	23	28	32	37	45	46
1.28	19	23	28	31	36	44	45
1.30	19	22	27	30	36	44	45

Depth-Width Ratio	Round	Rectangular with L/W Ratios as Shown					
	1	1	1.25	1.5	2.0	5	∞
1.32	18	22	27	30	35	43	44
1.34	18	21	26	29	34	43	44
1.36	17	21	25	29	34	42	43
1.38	17	20	24	28	33	42	42
1.40	16	20	24	28	32	41	42
1.42	16	19	24	27	32	41	41
1.44	15	19	23	27	31	40	41
1.46	15	18	23	26	31	39	40
1.48	15	18	22	25	30	39	40
1.50	14	18	22	25	29	38	39
1.85	10	13	17	19	22	30	33
1.90	10	12	16	18	21	30	32
1.95	9	11	15	16	20	29	31
2.00	9	11	15	15	19	28	30
2.25	8	10	13	15	18	27	29
2.10	8	10	13	15	18	27	29
2.15	8	9	12	14	17	26	28
2.20	7	9	12	14	16	26	28
2.25	7	9	12	14	16	26	27
2.30	7	8	1l	13	15	25	27
2.35	6	8	11	13	15	24	26
2.40	6	8	11	12	14	23	25
2.50	6	7	10	12	13	23	25
2.60	5	7	9	11	12	22	24
2.70	5	6	8	11	12	21	23
2.80		6	7	10	11	21	23

Depth-Width Ratio	Round	Rectangular with L/W Ratios as Shown					
	1	1	1.25	1.5	2.0	5	∞
2.90		5	6	9	1.0	20	22
3.00		5	6	8	10	19	21
3.50			5	6	7	16	18
4.00				4	5	14	16
4.50						12	14
5.00						11	13
5 50						10	11
6.00						10	11
6.50						9	10
7.00						8	9

In the particular case that p is 4000 psf, oe is 20 ft., oh is 20 ft., ab is 60 ft., ad is 100 ft., and z is 40 ft., the stress is:

$$\sigma_z/4000 = 0.238 - 0.135 - 0.137 + 0.084 = 0.050$$

Thus, the vertical stress 200 psf.

The stress caused by a loaded area of any shape and subjected to any variation of vertical stress can be obtained by suitable manipulation of the influence values and areas though, of course, the solution becomes tedious for complex shapes or loadings. Because the solutions were obtained by integrating the point load equations, they apply theoretically to a foundation with a frictionless base and they do not account for any flexural strength for the foundation.

Computations for footing settlement typically utilize the stress directly beneath the center of the footing. For convenience, the influence factors for that case (uniform pressure, Boussinesq case) are tabulated in Table 8.2.

For a flexible rectangular footing, the deflection of the surface can be estimated by integrating the equation for the deflection of the surface due to a point load. The surface deflection beneath the corner of a rectangular area is given by the following equation (Schleicher, 1926):

$$\Delta_z = \frac{pB}{\pi}\frac{1-\nu^2}{E}\left[\lambda \ln\left(\frac{1+\sqrt{1+\lambda^2}}{\lambda}\right) + \ln\left(\lambda + \sqrt{1+\lambda^2}\right)\right] \qquad (8.22)$$

where λ = L/B and L is the length of the rectangular footing and B is the width. Since the medium is assumed to be linearly elastic, the deflection of the surface at any point can be obtained by suitable additions and/or subtractions of stresses over rectangular areas with Eq.

8.22 applied for calculation of the settlement under one corner of each such area. The calculation is similar to that discussed for calculating vertical stresses using Eq. 8.21a. As a matter of convenience, the equation for surface deflection can be rewritten as:

$$\Delta_z = p\,B\,\frac{1-\nu^2}{E}\,I \qquad (8.23a)$$

where B is again the width of the rectangular footing and I is an influence factor. Values for the influence factor are presented in the following table for the center of the loaded area, centerline of the long edge, and corner, and for a rigid footing.

Vogt (1925, referenced by Giroud, 1968) gave solutions for the settlement of one corner of a square area subject to either uniform normal or shearing stresses. For the uniform shearing stress:

	Influence Factors				
L/B	**Center**	**Edge**	**Corner**	**Average**	**Rigid Footing**
1	1.12	0.76	0.56	0.95	0.82
2	1.53	1.12	0.76	1.30	1.12
5	2.10	1.68	1.05	1.82	1.6
10	2.56	2.10	1.28	2.24	2.0

$$\Delta_z = \tau\,B\,\frac{(1+\nu)(1-2\nu)}{E}\,0.18 \qquad (8.23b)$$

where τ is the shearing stress.

Giroud (1968a) presented influence factors for vertical surface displacements at various points under a loading diagram consisting of a frustrum of a pyramid with a rectangular base.

8.3.13 Newmark's method

The foregoing equations and tables can be used conveniently if the shape of the loaded area is geometrically simple. In some problems the surface loading may cover an area with irregular boundaries, or be discontinuous, or involve variable contact pressures, in which cases application of the foregoing procedures can lead to unnecessarily long calculations. In some of these cases, the most efficient method for estimating the stresses may be a graphical procedure developed by Newmark (1942, 1947).

The vertical normal stress at some point in the subsoil caused by a uniform stress applied over an area at the surface can be found from an equation such as: $\sigma_z = Ip$ where p is the uniform surface pressure and I is an influence factor which depends on the shape, position, and orientation of the loaded area, and the depth to the point where the stress is to be calculated. It is possible to subdivide the entire surface into areas such that each area has the same influence factor, i.e., so that the stress at the point in the soil equals the number of such areas that are loaded multiplied by the applied stress and the influence factor. A plan view of the surface, suitably subdivided, could be drawn to a proper scale and placed over a foundation plan and the number of loaded subdivisions of the surface then counted. It is

simpler, however, to prepare a single such influence diagram to a convenient scale and then prepare site plans at the required scales.

Such an influence diagram is shown in Fig. 8.14 (Newmark, 1942). A foundation plan is prepared to a scale F where:

$$F = s_d / s_f = L / z \tag{8.24}$$

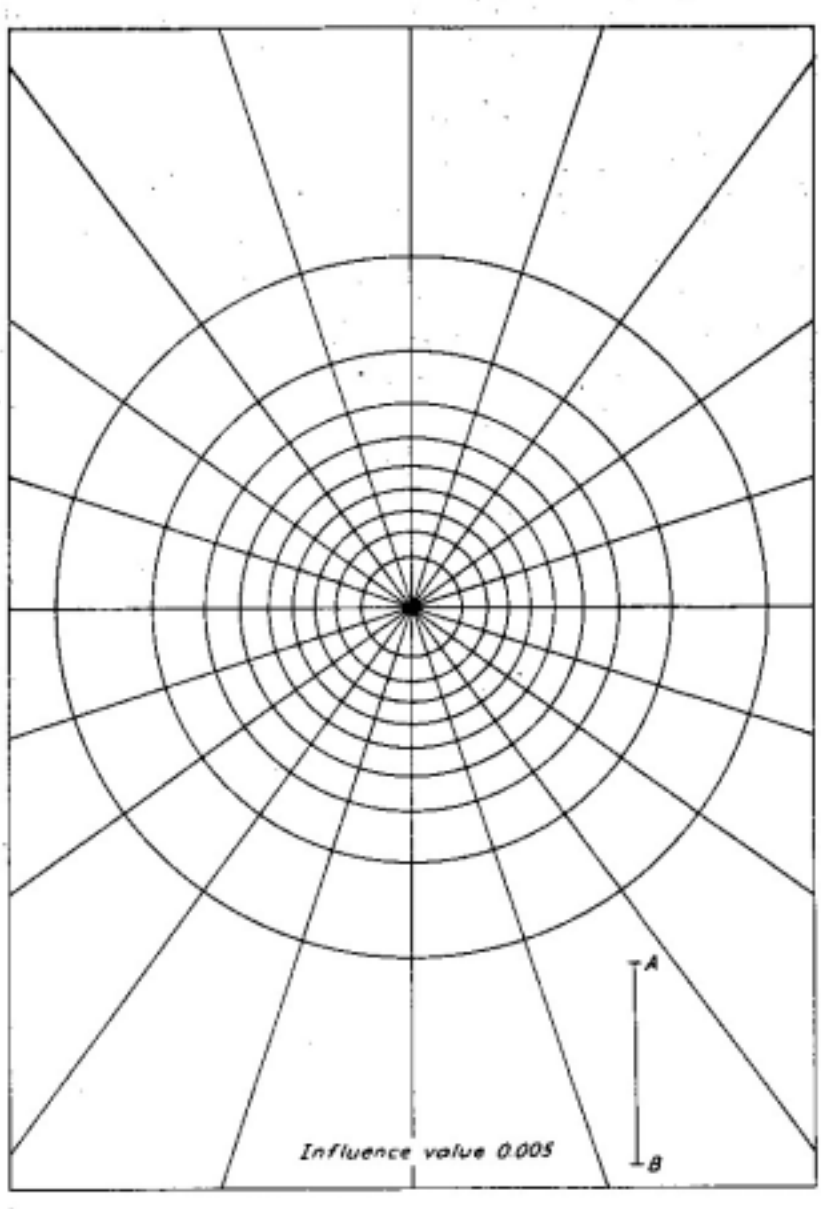

Fig. 8.14 Influence Chart for Computation of Vertical Stress Based on Boussinesq's Assumptions (after N. M. Newmark)

and s_d is a distance on the foundation plan view, s_f is a distance in the field, L is the length of the line shown on the influence diagram for scale, and z is the depth to the point where the stress is to be calculated. When using the diagram, the foundation plan view is drawn to the scale given by Eq. 8.24, placed over the influence diagram so that the point where the stress

is to be calculated lies directly under the center of the influence diagram, and the number of subdivisions of the influence diagram that are covered by the foundations are counted. The vertical stress at the point is then the multiple of the influence factor, the number of subdivisions covered, and the average applied pressure. Thus, if the influence factor is 0.002 and a 5000 psf surface loading covers 20 of the subdivisions, the induced vertical pressure is (20) (0.002) (5000) = 200 psf. The induced vertical pressure at any other position at the same depth is found in the same manner just by shifting the position of the foundation plan on the influence diagram and counting covered subdivisions again.

If there are N different pressures applied at the surface, then:

$$\sigma_z = \sum_{j=1}^{N} n_j p_j I \qquad (8.25)$$

where n_j indicates the number of subdivisions of the influence diagram covered by the foundations applying the pressure p_j.

If stresses are to be calculated at k different depths, it is necessary to prepare k different foundation plans, each drawn to the appropriate scale.

Since the boundaries of the surface loading are unlikely to match, precisely, the boundaries of the subdivisions in the influence diagram, it is necessary to estimate the percentage of some of the subdivisions that are covered. The accuracy of this procedure is improved by using charts with many surface subdivisions, and small influence factors, but the time involved in the counting procedure also increases.

Newmark (1942, 1947) presented charts that allow all stresses and deflections to be calculated.

8.3.14 Saint Venant's Principle

According to Saint Venant's principle, a complex distribution of applied stress (or deformation) can be replaced by a simpler one, for the purpose of simplifying the calculations, provided the stresses are calculated at points sufficiently far removed from the area where the stresses are applied. Thus, if a uniformly loaded circular area is treated as a point load for purposes of analysis, the error in the calculated value of σ_z will be large near the point load but will diminish with distance. The problem is to determine how far the point in the soil must be from the stressed area before the error becomes acceptably small. The distance depends on the size of the error considered acceptable and on the difference between the real applied stresses and the idealized loading.

The magnitude of the errors can be estimated by comparing the stresses caused by several different idealizations of the applied stresses. For example, the vertical normal stress induced in an elastic half space by a stress, p, applied uniformly over a square area of dimensions SxS can be compared with the stresses produced by a point load of magnitude $P = pS^2$ placed at the center of the area occupied by the square footing. If σ_{zS} is the stress caused by the square footing and σ_{zP} is the stress caused by the point load, then the error involved in assuming the stress applied by the square footing and the point load are equal may be defined as:

$$E_1 = \frac{\sigma_{zp} - \sigma_{zs}}{p}$$

This error is plotted versus depth in Fig. 15a for points beneath the center of the square footing, under the centerline of an edge, and under a point a distance of 0.5S out from the centerline of an edge. Apparently, the error is negligible for depths greater than twice the footing width (see also Krynine, 1936).

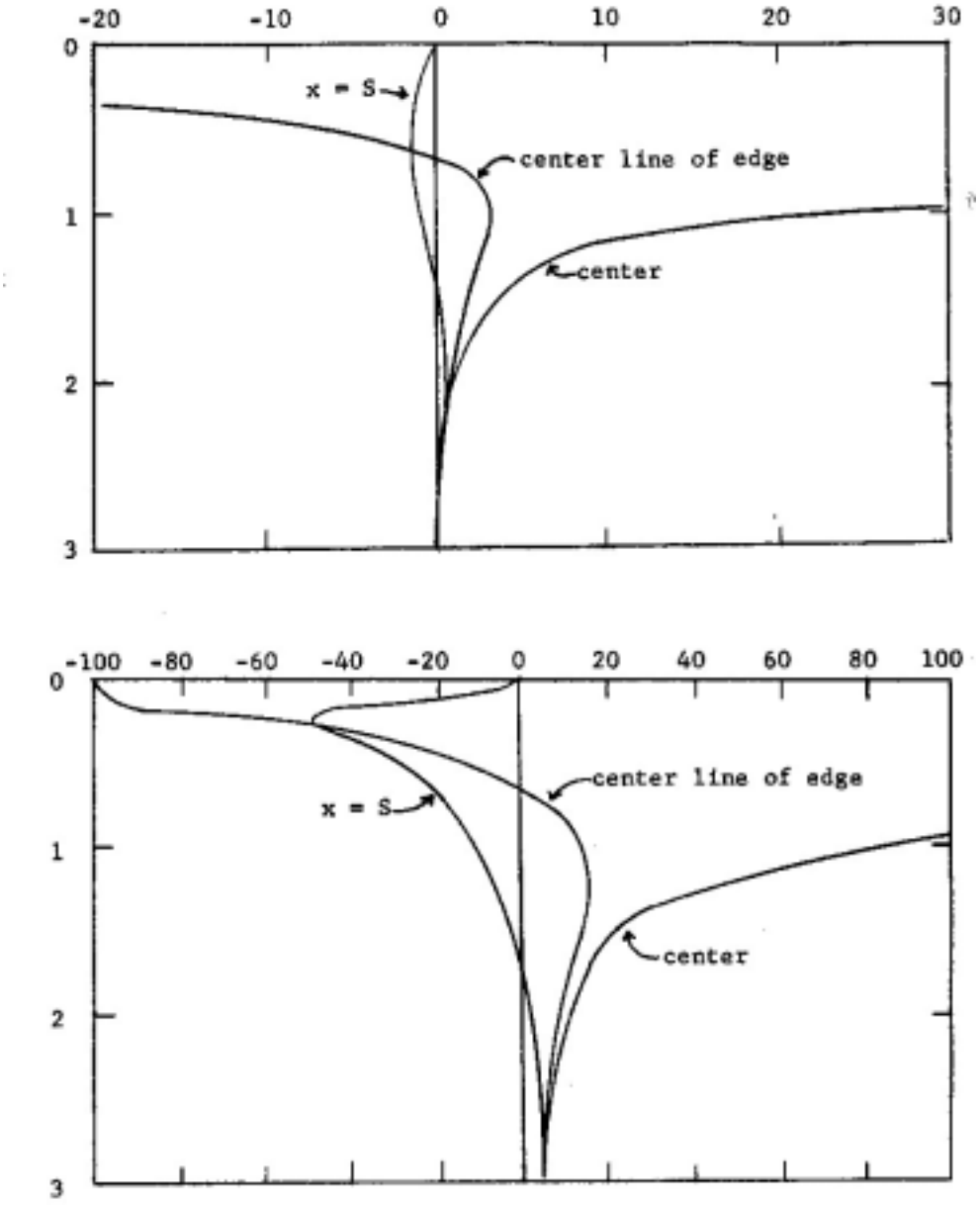

Fig 8.15 Spatial Distribution of the Error in Vertical Normal Stress that Results from the Assumptions that the Uniform Pressure on a Square Footing of Width S can be Replaced by a Point Load of Magnitude qS^2 where q is the Uniform Footing Pressure

In cases where the stress caused by a number of foundations are to be determined, it may be of interest to know the error in terms of the proper stress at that depth, i.e.:

$$E_2 = \frac{\sigma_{zp} - \sigma_{zs}}{\sigma_{zs}}$$

This error is shown in Fig. 15b. For most practical work this error would seem to be tolerable for depths greater than two or three times the width of the footing.

In a similar manner it can be shown that a line load is an excellent approximation for a uniformly loaded strip for depths greater than two or three times the width of the strip.

Of course, the stress applied to the soil by real footings is unlikely to be uniform. The actual contact stress may be peaked up in the middle, at the edge, or at some intermediate point. If the stress is peaked up at the middle, then the error involved in use of point or line load approximations is even smaller than discussed previously. If the stress is concentrated at the edge of the footings, the error is larger. To determine the limiting error it may be assumed that all of the load is transmitted to the soil at the periphery of the footing, i.e., by a line load. If the footing has dimensions of SxS and carries a
total force P, then the difference between the vertical compressive stresses calculated for the line load around the outer edge of the footing and a central point load, expressed in terms of $p = P/S^2$, is less than 3% at a depth of 2S and less than 1% at 3S.

Based on these calculations it would appear economically justified to perform stress calculations by replacing footings with point loads, and long strip loads by line loads, provided that stresses are to be calculated at depths greater than about two or three times the smaller dimension of the loaded area, the depth depending on the acceptable error.

It is important to note that the "errors" discussed in this section represent differences between two theoretical solutions, for both of which the soil is assumed to be a homogeneous, isotropic, weightless, semiinfinite, linearly elastic, continuum with a plane horizontal surface subjected to normal stresses. For practical work the error of interest is the difference between the real stress and the calculated stress, an error whose magnitude depends on the accuracy of the foregoing assumptions.

In cases where the contact stress between a footing and the subsoil is complex, it may be convenient to consider the contact stresses as a series of point or line loads, or to use some other simplified pattern of load. Saint Venant's principle is applied to determine reasonable spacings of these loads in terms of the depth where the stresses are to be calculated.

In some rare cases it becomes necessary to determine settlements of mat foundations that are relatively flexible and subjected to concentrated loads. The actual distribution of contact stresses is unknown. A distribution may be assumed, and stresses in the subsoil calculated as just described, and then the resulting settlements calculated. These settlements are then used to determine the resulting redistributions of load in the superstructure, and a new distribution of contact stresses is calculated. After several such iterations, contact stresses may be obtained that are compatible with the properties of the superstructure and the subsoil.

With such nonuniform contact stresses, rigorous solutions even for a highly idealized "soil" are unlikely, and Saint Venant's principle must usually be applied to simplify the calculations.

8.4 Homogeneous, Anisotropic, Weightless, Linearly Elastic Half Spaces with Plane Horizontal Surfaces

Although the assumptions are usually made that the soil is homogeneous and isotropic, it is apparent that most field problems involve soils that are stratified and anisotropic. Naturally, the question arises as to the size of the errors associated with the assumptions of uniformity in the soil. These errors can be studied either experimentally or analytically. In this section consideration will be restricted to the theoretical studies.

8.4.1 Westergaard's analysis

Westergaard (1938) investigated the problem of a finely stratified soil in which certain of the strata were so strong that they prevented lateral deformations of significant magnitude anywhere in the soil. To make the problem mathematically tractible, he assumed that the soil consisted of a homogeneous, isotropic, weightless, linearly elastic material horizontally reinforced by inextensible membranes of negligible thickness and spaced very closely together. The membranes completely prevented lateral deformation in the uniform material but occupied a negligible volume. He presented solutions for a vertical point load at the surface and at some depth within the medium, and discussed the stress functions for plane strain problems.

The equation for the vertical normal stress, σ_z, caused by a vertical point load at the surface can be put into the form:

$$\sigma_z = I \frac{P}{z^2} \tag{8.26}$$

where I is an influence factor, P is the point load, and z is depth. In Table 2, influence factors are tabulated for a range of values of (r/z) and Poisson's ratio and are compared with the equivalent influence factor from Boussinesq's equation for an isotropic medium. If the assumption is made that Poisson's ratio for a saturated soil, loaded under undrained conditions, is 0.5, then the influence factor directly beneath the point load is infinite at all depths. Thus, for a stress distributed over a small area at the surface, the induced vertical normal stresses in the soil would be severely peaked up compared with the stresses for an isotropic medium. Conversely, if Poisson's ratio is assumed to be low, then the vertical compressive stress is spread out compared with that found for an isotropic medium.

Table 8.3. Comparison of Influence Factors for Vertical Compressive Stress Induced by a Vertical Point Load Applied at the Surface, Calculated using the Equations of Boussinesq and Westergaard

	Influence Factors, $\sigma_z z^2/P$			
		Westergaard		
r/z	Boussinesq	ν=0	ν=0.3	ν=0.49
0.0	0.48	0.32	0.56	8.04
0.2	0.43	0.28	0.46	1.53
0.5	0.27	0.17	0.22	0.16
1.0	0.08	0.06	0.06	0.02
2.0	0.01	0.01	0.01	0.00

Influence factors were developed for the vertical compressive stress beneath: (l) a vertical point load, (2) one end of a line load of finite length, (3) the center of a circular area subjected to a uniform stress, and (4) one corner of a uniformly loaded rectangular area, by Fadum (1948) for the unlikely case that Poisson's ratio was zero.

Poisson's ratio for saturated soils loaded under undrained conditions is likely to be nearer 0.5 than zero. Thus, the assumption of a value of zero must be looked upon with some skepticism. Further, it is not apparent that there are a significant number of field problems in which Westergaard's assumptions have any applicability. It was supposed that they would apply to soft clays in which interspersed thin layers of sand would simulate the membranes but it is not apparent how sand layers of negligible tensile strength can act as inextensible membranes even after superimposing the initial stresses on the system. Even buried desiccated clay layers are unlikely to act as inextensible membranes because they are likely to be fissured. Thus, it appears that the assumptions made in Westergaard's analysis have little application in foundation engineering and the values of Poisson's ratio usually assumed by engineers who use Westergaard's theory are unlikely to be correct.

8.4.2 Two dimensional anisotropy

The phrase "two dimensional anisotropy" is used here to indicate that the anisotropy can be expressed in two dimensions rather than three. Specifically, consideration is restricted to the case generally encountered with natural soil deposits in which the properties in the horizontal directions differ from those in the vertical direction.

Solutions for the stresses and deformations caused by a vertical point load applied at the surface have been presented by Koning (1957) and Barden (1963). The equations are too lengthy either to be presented here or to be used in normal engineering practice. Further, they require numerical values for three different Poisson's ratios and two Young's moduli. Evaluation of these constants for practical problems would be exceedingly difficult. Nevertheless, numerical evaluation of the equations for ranges of values of the various constants leads to qualitative conclusions of general interest. The vertical normal stress, $_z$, is found to be influenced strongly by the ratio of the horizontal to vertical values of Young's modulus, E_h/E_v but not by the values of Poisson's ratios to any great extent (Barden, 1963). Let F designate the ratio of $_z$ for the anisotropic medium to the value for an isotropic medium. For the stresses in the medium directly beneath the point load the average relationship between F and E_h/E_v is as follows:

E_h/E_v	1/4	1/2	1	2	4	6	infinite
F	1.94	1.19	1.00	0.83	0.60	0.50	0.33

Thus, for soils with E_h exceeding E_v, i.e., for highly overconsolidated clays or very dense sands, the vertical compressive stress tends to be spread out and the maximum value of this stress beneath a point load is smaller than the value calculated using Boussinesq's equation. For normally consolidated clays and loose sands, E_h is probably less than E_v and the vertical normal stresses are slightly peaked up. However, for the range of values of E_h/E_v likely to be encountered in engineering practice, and for distributed loads, it appears that the "error" involved in using the Boussinesq solutions will be much smaller than the "error" resulting from such uncertainties as the magnitudes of the applied load, the distribution of load across a foundation, or the influence of soil stratification.

8.5 Multi-Layered Systems in which Each Layer is Homogeneous, Isotropic, Weightless, and Linearly Elastic

8.5.1 Introduction

Because of the manner in which they are formed, most soil deposits are stratified with the boundaries between strata generally horizontal. Thus, instead of treating the soil as homogeneous it should be treated as a system of horizontal layers. As a first approximation each layer may be considered homogeneous, isotropic, weightless, and linearly elastic, and the properties defined using two coefficients. The variables to be considered then include the elastic properties of the layers, the distribution of stresses or deformations at the boundary, the relative thicknesses of the layers, and the conditions of continuity at the interfaces between layers. It is apparent that presentation of tables or figures giving the various stresses and deformations for suitable ranges in the afore mentioned variables is not feasible. Further, even presentation of the solutions in the form of equations is difficult because the equations must usually be left in the form of integrals that are evaluated numerically for each specific problem. As a result of these problems the following discussion will apply only to relatively simple cases. References will be made to the original papers in which more detailed discussions are presented.

8.5.2 Elastic layer on a rigid base

The simplest multi-layered system consists of a homogeneous, isotropic, linearly elastic layer overlying a rigid base. The base is a half space with a plane horizontal surface. The interface between the elastic layer and the rigid base may be considered "smooth" or "rough." A smooth interface is defined to be one in which the shearing stresses are zero; the radial deformations are discontinuous at the interface. A rough interface is defined to be one in which the radial deformations of the two layers are equal and shearing stresses are developed in the interface. For a rough rigid base, the horizontal deformations at the interface must be zero.

Biot (1935) presented solutions for the vertical normal stress at the interface for a surface point load and surface line load of infinite length, both for a smooth and a rough interface.* For the smooth interface the vertical normal stress was independent of Poisson's ratio. For the rough interface Biot's solutions are valid only for Poisson's ratio equal to 0.5. The vertical normal stress acting at the interface at a depth of h, directly under the surface loading, is as follows:

---

* Previous correct solutions for the case of a smooth interface were presented by Filon (1903), Carothers (1924), and Timoshenko (1934). For the rough interface, the first solutions were presented by Carothers (1924b) and extended by Jurgenson (1934, 1936). Passar (1935) demonstrated that Carothers's solutions were incorrect, thus invalidating Jurgenson's solutions as well. Passar (1935) presented correct solutions for a vertical point load and Marguerre (1931, 1933) presented solutions for plane stress and axially symmetrical cases but their "solutions" were left in the form of integrals and were correct only for Poisson's ratio equal to zero. Subsequently Pickett (1938) presented solutions for point and line loads, together with numerical results. Holl (1939) pointed out that Pickett 's solutions are in error except for the case the Poisson's ratio is 0.5. Holl presented solutions for a variety of plane strain problems but they were in the form of integrals.

Loading	Case	Vertical Normal Stress at the Interface Beneath the Surface Loading
Point Load	Boussinesq	$(3P/2\pi h^2)$
	Smooth Interface	$1.711\ (3P/2\pi h^2)$
	Rough Interface	$1.557\ (3P/2\pi h^2)$
Infinite Line Load	Boussinesq	$(2p/\pi h)$
	Smooth Interface	$1.441\ (2p/\pi h)$
	Rough Interface	$1.291\ (2p/\pi h)$

where the "Boussinesq" case is for an elastic half space without an interface and is used for comparison with the solutions for the rigid base, P is the point load, and p is the line load in units of force per unit length. Biot's solutions demonstrate that the vertical normal stress tends to be peaked up on the rigid base, compared to the Boussinesq case, and that the peaking is more severe for the smooth base than for a rough base. The error involved in applying Boussinesq's equations to cases involving a rigid base is apparently a maximum for the vertical point load, smaller for the line load of infinite length, and zero for the case of an infinitely extended uniform surface pressure.

Cummings (1941) found the vertical normal stress acting on a rough interface at a depth h beneath the center of a uniformly loaded circular area by integrating Biot's solution for a point load. He found that the vertical normal stress exceeded the stress in a semi-infinite homogeneous body (the Boussinesq case) by 0% for h/R = 0, 30% for h/R = 1, 50% for h/R = 2, and by an amount approaching 56% as h/R increased further (St. Venant's Principle).

Burmister (1956) presented equations, in the form of integrals, for all the pertinent stresses and deformations within the elastic upper layer on a rigid base with a rough interface for Poisson's ratio of 0.4. He presented numerical solutions in the form of influence diagrams for the vertical compressive stress beneath one corner of a uniformly loaded rectangular area and for the settlement of the surface, and Newmark-type charts for various stresses and deformations. His calculations confirm the differences between the exact solutions and the Boussinesq solutions previously discussed.

8.5.3 Two elastic layers

The two-elastic-layer system consists of a surface layer of uniform finite thickness overlying a layer of infinite depth. Both layers extend indefinitely in the horizontal directions. They are assumed to be homogeneous, isotropic, weightless, and linearly elastic. The interface may be smooth or rough.

This system has been analyzed by Burmister (1943, 1945, 1956), Fox (1948a, 1948b), Mehta and Veletsos (1959), and others. The analyses generally apply to either a point load or a load uniformly distributed over a circular area, both at the upper surface. Exact solutions can be obtained for stresses and deformations under the centerline of the load whereas numerical methods are used to find stresses and deformations at other points.

The effect of stratification on the vertical normal stresses can be demonstrated using the solutions presented by Fox (1948b). The loading is a uniform stress applied over a circular area of radius R. The two layers have Poisson's ratios of 0.5. Young's modulii are E_1 for the

upper layer and E_2 for the lower one. As a matter of convenience, let F designate the ratio of the vertical normal stress in the two-layer system to the stress in a single homogeneous layer of infinite extent (the Boussinesq case). Values of F are given in the following table for the interface between the two layers at a point beneath the center of the circular area. The thickness of the upper layer is h.

h/R	E_1/E_2	F (%)	
		Smooth Interface	Rough Interface
1/2	1	110	100
	10	74	71
	100	27	27
	1000	7	8
1	1	112	100
	10	47	45
	100	13	13
	1000	3	3
2	1	109	100
	10	37	35
	100	8	8
	1000	2	2

The vertical normal stresses under the centerline at the interface are slightly higher for a smooth interface than for a rough one but the difference is too small to be of practical engineering significance. The effect of a surface layer of high Young's modulus is apparently to spread the vertical normal stresses over a wider area than for the case of a single homogeneous layer.

Solutions of the foregoing type are of value in foundation engineering because they indicate, qualitatively, the effects of surface sand layers, compacted fills, or desiccated crusts on the stresses in the underlying more compressible soils. The equations are only of qualitative use, not only because the soils do not meet the assumptions of the theory, a problem that occurs with all the solutions in which the theory of elasticity is used, but because of the difficulty in assigning reasonable values to the ratios E_l/E_2 and $_l/\ _2$. Field data are needed before the solutions can be used ln engineering design with reasonable confidence.

8.6 Field And Laboratory Obsevations

8.6.1 Introduction

The mathematical analyses previously considered all apply to idealized systems which never precisely duplicate conditions in nature. Use of these analyses in engineering practice is justified only if actual experimental measurements can be used to indicate the nature and size of the errors caused by the idealizations. Unfortunately, the expense and technical difficulties associated with the collection of such data are so severe that very few reliable field

observations are available. Most of the available observations are for soils prepared in the laboratory.

It is convenient to consider the experimental observations in three groups according to soil conditions, viz: (l) homogeneous sands, (2) homogeneous clays, and (3) layered soil systems.

8.6.2 Observations with sandy soils

Cummings (1936) summarized the experimental measurements of the vertical normal stress induced in sand that had been reported by Steiner-Kick (1879), Strohschneider (1909), Goldbeck (1917), Enger (1920, 1929), and Kogler and Scheidig (1927, 1929). These investigators had applied loads to the surface of compacted specimens of sand using rigid circular plates with diameters ranging from 0.6" to 36". They measured the vertical normal stresses at various points on the floors of the vessels that contained the sand, using a variety of types of load cells. The influence of depth on the vertical normal stress was evaluated by varying the depth of sand in the container.

The reported values of the vertical normal stress directly beneath the centerline of the loading discs are plotted versus depth in Fig. 8.16. The measured stresses are considerably higher than the calculated values, especially at shallow depths, when a Boussinesq distribution was used with a uniform footing pressure. The equations for the contact stress between a rigid disc and an elastic body cannot be used to correct the stresses because these equations predict infinite edge stresses, an impossible situation, especially with a dry sand.

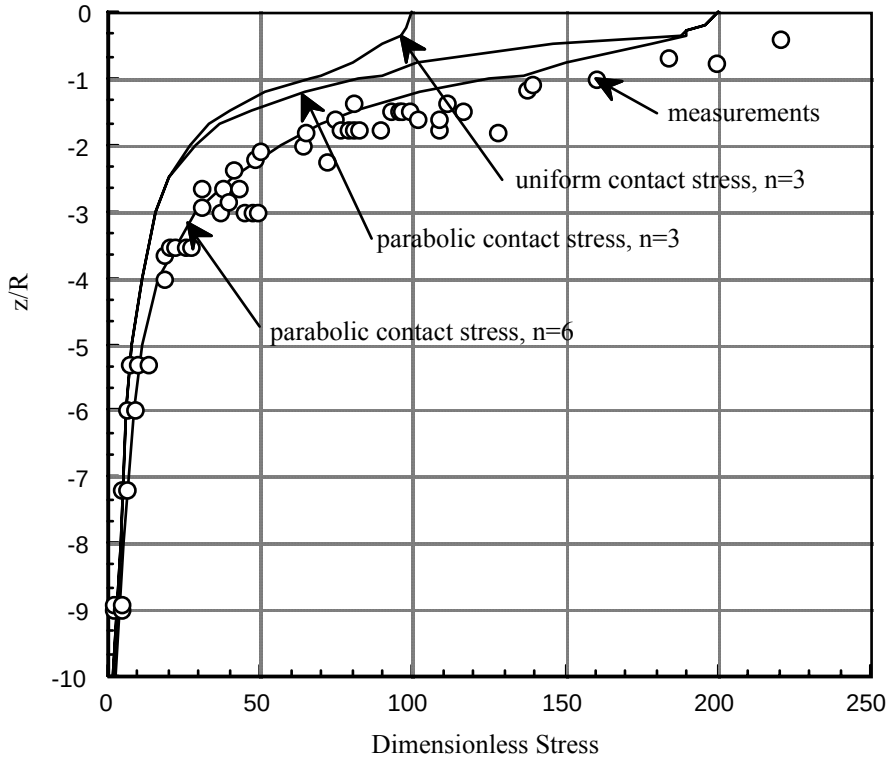

Fig. 8.16 Distribution of the Vertical Normal Stress with Respect to Depth Beneath the Centerline of a Surface Rigid Disk Subject to Normal Force

Farber (1933) measured the contact stresses between reasonably rigid circular plates and

bodies of sand. The contact stresses shown in Fig. 8.17 are typical of his data. The actual contact stresses are apparently nearly parabolic with the maximum stress in the center. This distribution of contact stress results from the lateral extrusion of the relatively unconfined sand from under the periphery of the rigid loading plate, thus concentrating the stress under the center. The soil near the edges of the plate is apparently in a state of plastic equilibrium. However, in order to perform the analysis, the sand is assumed to remain elastic and the contact stress is assumed to vary parabolically from zero at the edge to twice the average contact stress at the center. The correct equation for this case was given by Krynine (1936):

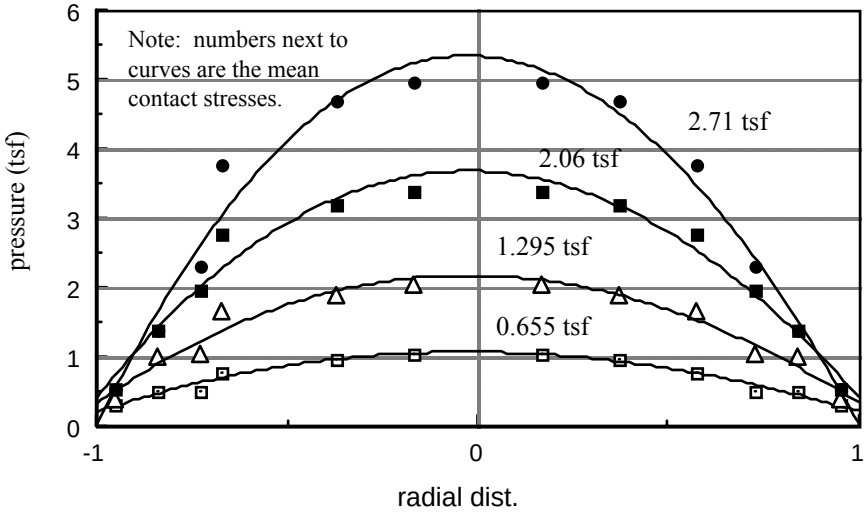

Fig. 17 Distribution of Normal Contact Stress Over the Base of a Rigid Circular Footing at the Surface of Dry Sand. The solid lines are fitted cubic curves.

$$\sigma_z\,(r=0) = 2p\left[1 - 2\alpha^2 + \frac{2\alpha^3}{\sqrt{1+\alpha^2}}\right] \qquad (8.27)$$

in which $\sigma_z\,(r=0)$ is the vertical normal stress at some depth z beneath the center line, p is the average value of the contact stress, $\alpha = z/R$, and R is the radius of the loading plate. The stress defined from Eq. 27 is also plotted versus depth in Fig. 16 (n=3). The correlation between theory and measurement is much improved but the measured stresses still exceed the calculated values.

Griffith (1929) and Frohlich (1932) independently concluded that the assumptions of Boussinesq's theory were not really applicable to sands and suggested rewriting his equation for the vertical normal stress induced by a surface vertical point load in the form:

$$\sigma_z = \frac{nP}{2\pi R^2}\left(\frac{z}{R}\right)^n \qquad (8.28)$$

where all symbols are as defined for Eq. 8.1 except for n which is termed the concentration factor n. If n is 3 then Eq. 28 reduces to Boussinesq 's equation. Griffith and Frohlich suggested that in dense sands n might be as great as 6. It may be noted that Eq. 8.28 does not satisfy all the requirements from the theory of elasticity unless n is 3. The justification for

using Eq. 8.28 is a pragmatic one, not a theoretical one.

Equation 8.28 may be integrated to find the stress at any depth beneath the center line of a disc. For a uniform contact pressure the stress is:

$$\sigma_z(r=0) = p\left[1 - \frac{\alpha^n}{(1+\alpha^2)^{n/2}}\right] \tag{8.29}$$

For a parabolic distribution of contact pressure:

$$\sigma_z(r=0) = 2p\left[1 + \frac{2}{2-n}\alpha^2 - \frac{2}{2-n}\,\alpha^n\,(1+\alpha^2)^{\frac{2-n}{n}}\right] \tag{8.30}$$

Equation 8.30 was used to calculate the curve in Fig. 8.16 with n=6. The laboratory measurements approximate this latter curve better than any of the other curves. The correlation can be improved further by assuming some other distribution of contact stress, e.g. Eremin (1936) presented a solution for a conical distribution and n = 3.

The pressures used in Fig. 8.16 were measured in the rigid floors of the test vessels. Thus, Biot 's (1935) equations should be used to determine the normal stresses. Biot's equation for a rough rigid base was integrated to find the vertical normal stress on the base directly beneath the center of a uniformly loaded disc by Cummings (1941). The resulting equation is too long to be presented. However, it demonstrated that the vertical normal stress at various depths under the centerline was increased by an amount ranging from zero at the surface to 56% for depths greater than about 3R. The stresses are nearly equal to those calculated for a uniform contact stress, a semi-infinite soil, and a concentration factor of 5. No solution has been obtained for the case of a parabolic contact stress and a rigid base, based on Biot's point load equation, but it can be seen that the resulting curve should be similar to the curve with n=6 in Fig. 8.16.

A series of stress measurements were made at the Waterways Experiment Station (WES, 1954) with load cells buried within sand specimens. The specimens were 48 feet long, 32 feet wide, and up to 9 feet deep. Uniform pressures of 15, 30, and 60 psi were applied at the surface over circular areas of 250, 500, and 1000 sq. in. (diameters of about 18, 25, and 36 in.). Stresses and deformations were measured in various directions and in various locations under single circular loaded areas and under pairs of circular loaded areas with various center-to-center spacings. The vertical normal stresses measured under the center lines of the loads are shown as a function of depth in Fig. 8.18. At measured stresses are slightly greater than those calculated with Boussinesq's theory especially at shallow depths. However, integration of the measured stresses showed over-registration at shallow depths and under-registration at greater depths. An adjustment for the influence of the gages on the stresses would appear to bring measured stresses into excellent agreement with the theoretical stresses. There is no need to invoke a concentration factor greater than three.

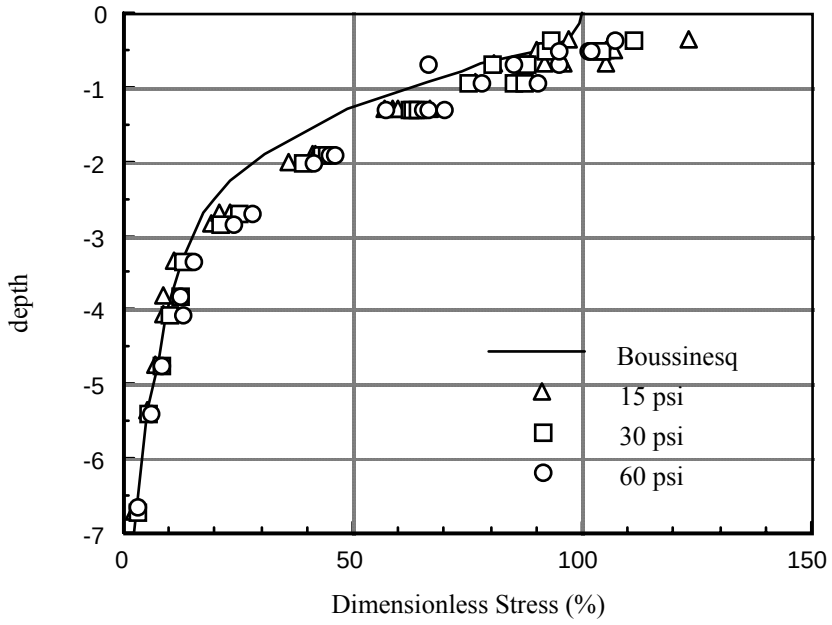

Fig. 8.18 Comparison of Measured and Computed Stresses within a Body of Sand

Based on these observations it is apparent that variations in the contact pressure across the base of a footing can be important and that non-uniform pressures may be expected for rigid footings. For the dense sands used in the experiments and for surface loading with a rigid disc, the contact pressure varies from close to zero at the edge of the disc to a maximum at the center. Further, to make the experimental data and theoretical curves coincide it is necessary to account for the rigid base and also perhaps to arbitrarily introduce the concentration factor whose value is apparently about 6 for the cases under consideration. Lower values for the concentration factor may be required when loose sands are encountered. For a uniform applied stress the measured vertical normal stresses compare very well with the stresses calculated using Boussinesq's theory.

Some of the discrepancy between measured and computed stresses may result from over- or under-registration by the load cells. However, most of the investigators integrated the measured stresses to find the total force registered by the gages. This calculated force generally compared well with the known applied force, thus suggesting that the gages were operating properly.

8.6.3 Observations in clays

There are only limited data on measured stresses in clay, and then only for compacted clays. There is no convenient way of inserting a load cell into a natural clay without causing severe stress redistribution problems. The best set of data seems to have been collected in a study at the Waterways Experiment Station (Foster and Fergus, 1951). They used a sample that was 26 feet square and 12 feet deep. They compacted the sample with load cells at one elevation. They used 12-inch diameter WES cells. Loads were applied on the surface to represent tire pressures and stresses were measured. The load cells were mounted at a single elevation low in the test specimen. After the first set of measurements, some of the soil was planed off to reduce the distance from the loads to the load cells, and another set of readings was made. The process was repeated to obtain information on the spatial variation

in developed pressures. This procedure reduced the number of load cells required for the experiments and left the load cells in the same soil throughout.

Numerous plots of measured and computed stress were developed. An example plot in shown in Fig. 8.19 for the case of loading from a dual landing gear with a center-to-center spacing of the tires of 7.5 feet. Measurements were made for loads of 15,000, 30,000, 45000, and 60000 pounds. The data in Fig. 8.19 are typical of numerous other plots. The data suggest that Boussinesq's theory is adequately accurate, at least for compacted clays.

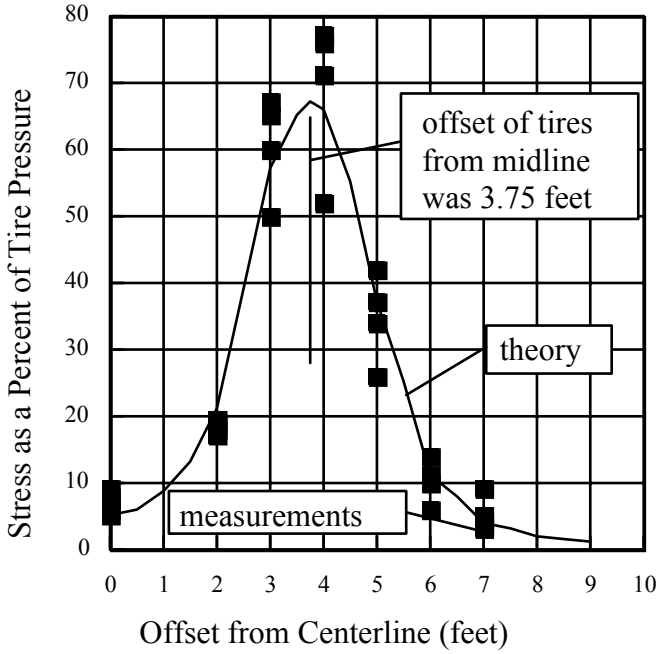

Fig. 8.19 Comparison of Measured and Computed Vertical Stresses for the Case of a Dual Landing Gear Loading, and Stresses at a Depth of One Foot (Foster and Fergus, 1951, p. 11).

8.7 References on Stresses and Displacements in Elastic Media

Acum, W. E. A. and L. Fox (1951), "Computation of Load Stresses in a Three Layer Elastic System," *Geotechnique*, Vol. 2, pp. 293-300.

Ahlvin, R. E. and H. H. Ulery (1962), "Tabulated Values for Determining the Complete Pattern of Stresses, Strains, and Deflections Beneath a Uniform Circular Load on a Homogeneous Half Space," *Highway Research Bulletin No. 342, Stress Distribution in Earth Masses*, pp. 1-13.

Barber, E. S. (1963), "Shear Loads on Pavements," *Proceedings, International Conference on the Structural Design of Asphalt Pavements*, Univ. of Michigan.

Bishop, A. W. (1952), "The Stability of Earth Dams," Ph.D. Thesis, University of London.

Biot, M. A. (1935), "Effect of Certain Discontinuities on the Pressure Distribution in a Loaded Soil," *Physics*, Vol. 6, pp. 367-375.

Boussinesq, M. J. (1885), "Application des potentiels a l'etude de l'equilibre et du mouvement des solides elastiques, principalement au calcul des deformations et des pressions que produisent, dans ces solides, des efforts quelconques exerces sur une petite partie de leur surface ou de leur interieur: Memoire suivi de notes etendues sur divers points de physique mathematique et d'analyse," GauthierVillars, Paris, pp. 722.

Buisman, A. S. (1932), "Druckverdeeling in Bouwgrond in Verband met Ongelijke Samendrukbaarheid in Horizontale en Verticale Richting," *De Ingenieur*, Vol. 45, pp. 175-180.

Burmister, D. M. (1938), "Graphical Distribution of Vertical Pressure Beneath Foundations," *Transactions*, ASCE, Vol. 103, pp. 303-343.

Burmister, D. M. (1943), "The Theory of Stresses and Displacements in Layered Systems and Application to the Design of Airport Runways," *Proceedings,* Highway Research Board, Vol. 23, pp. 126-148.

Burmister, D. M. (1945), "General Theory of Stresses and Displacements in Layered Systems," *Journal of Applied Physics*, Vol. 16, No. 2, pp. 39-96; No. 3, pp. 126-127; No. 5, pp. 296-302.

Burmister, D. M. (1956), "Stress and Displacement Characteristics of a Two-Layered Rigid Base Soil System: Influence Diagrams and Practical Applications," *Proceedings,* Highway Research Board, Vol. 35, pp. 773-814.

Burmister, D. M. (1958), "Evaluation of the Pavement Systems of the WASHO Road Test by Layered System Methods," *Highway Research Board Bulletin 177*.

Burmister, Donald M. (1962a), "Applications of Layered System Concepts and Principles to Interpretations and Evaluations of Asphalt Pavement Performances and to Design and Construction," *International Conference on Structural Design of Asphalt Pavements,* Univ. of Michigan, pp. 441-453.

Burmister, Donald M. (1962b), "Applications of Layered System Concepts to Design and Construction of Asphalt Pavement," *Proceedings,* First Paving Conf., Univ. of New Mexico, Albuquerque, pp. 147-184.

Burmister, Donald M. (1963), "Layered System Design as Applied to Concrete Pavements," *Proceedings*, Second Paving Conf., Univ. of New Mexico, Albuquerque, pp. 21-47.

Burmister, Donald M. (1965), "Influence Diagrams for Stresses and Displacements in a Two-Layer Pavement System for Airfields, Part I," project report from the Department of Civil Engineering and Engineering Mechanics, Columbia University, to the Department of the Navy, Bur. of Yards and Docks, Wash., D. C., Contract NBy 13009, 66 pp.

Carothers, S. D. (1924a), "The Elastic Equivalence of Statically Equipollent Loads," *Proceedings*, Intern. Mathematical Congress, Toronto, Vol. 11, pp. 519-526.

Carothers, S. D. (1924b), "Test Loads on Foundations as Affected by Scale of Tested Area, "

Proceedings, Intern. Mathematical Congress, Toronto, Vol. 11, pp. 527-549.

Cerruti, Valentino (1882), "Ricerche intorno all' equilibrio de'corpi elastici isotropi, " *Reale Accademia dei Lincei, Memorie della Classe di Scienze Fisiche, Matematiche et Naturali*, Ser. 3a, Vol. 13, pp. 81-122, Roma.

Christensen, C. B. (1950), "Geostatic Investigations with Especial Reference to Embankment Sections," *Ingeniorvidenskabelige Skrifer*, Vol. 3, Copenhagen.

Cummings, A. E. (1936), "Distribution of Stresses Under a Foundation," *Transactions*, ASCE, Vol. 101, pp. 1072-1134.

Curtis, A. J. and F. E. Richart (1955), "Photoelastic Analogy for Nonhomogeneous Foundations," *Transactions,* ASCE, Vol. 120, pp. 35-53.

Davis, E. H. and H. Taylor (1961), "The Surface Displacement of an Elastic Layer Due to Horizontal and Vertical Surface Loading," *Proceedings, Fifth Intern. Conf. on Soil Mech. and Found. Engr.,* Vol. 1, pp. 621-628.

Deresiewicz, H. (1960), "The Half-Space Under Pressure Distributed Over an Elliptical Portion of Its Plane Boundary," *Journal of Applied Mechanics*, March.

Fadum, Ralph E. (1948), "Influence Values for Estimating Stresses in Elastic Foundations," *Proceedings, Sec. Intern. Conf. on Soil Mech. and Found. Engr.,* Vol. 3, pp. 77-84.

Fergus, S. M. and W. E. Miner (1955), "Distributed Loads on Elastic Foundation," *Proceedings, Highway Research Board*, Vol. 34, pp. 582-597.

Foster, C. R. and R. G. Ahlvin (1954), "Stresses and Deflections Induced by a Uniform Circular Load," *Proceedings, Highway Research Board*, Vol. 33, pp. 467-470.

Foster, C. R. and S. M. Fergus (1951), "Stress Distribution in a Homogeneous Soil," *Res. Report No. 12-F, Highway Research Board*, 36 pp.

Fox, L. (1948a), "Computation of Traffic Stresses in a Simple Road Structure," *Proceedings, Sec. Intern. Conf. on Soil Mech. and Found. Engr.*, Vol. 2, pp. 236-246.

Fox, L. (1948b), "Computation of Traffic Stresses in a Simple Road Structure," D.S.I.R. Road Res. Tech. Paper No. 9.

Gerrard, C. M. (1968), "The Axisymmetric Deformation of a Homogeneous, Cross-Anisotropic Elastic Half Space," *Highway Research Record*, No. 223, pp. 36-44.

Gibson, R. E. and J. McNamee (1957), "The Consolidation Settlement of a Load Uniformly Distributed Over a Rectangular Area," *Proceedings, Fourth Intern. Conf. on Soil Mech. and Found. Engr.*, Vol. 1, pp. 297-299.

Giroud, Jean-Pierre (1968a), "Settlement of an Embankment Resting on a Semi-Infinite Elastic Soil," *Highway Research Record*, No. 223, pp. 18-35.

Giroud, Jean-Pierre (1968b), "Settlement of a Linearly Loaded Rectangular Area,"

Proceedings ASCE, Vol. 94, SM4, pp. 813-831.

Gray, Hamilton (1936), "Stress Distribution in Elastic Solids," *Proceedings, Intern. Conf. on Soil Mech. and Found. Engr.*, Vol. 2, pp. 157-168, Cambridge.

Griffith, J. H. (1929), "The Pressure Under Substructures," *Engr. and Contr.,* Vol. 1, pp. 113-119.

Hank, R. J. and F. H. Scrivner (1948), "Some Numerical Solutions of Stresses in Two and Three Layered Systems," *Proceedings, Highway Research Board,* Vol. 28, pp. 449-468.

Harr, Milton E. and Charles W. Lovell, Jr. (1963), "Vertical Stresses Under Certain Axisymmetrical Loadings," *Highway Research Record*, No. 39, pp. 68-77.

Hogg, A. H. H. (1938), "Equilibrium of a Thin Plate Symmetrically Loaded, Resting on an Elastic Foundation of Infinite Depth," *Phil. Mag*., Vol. 25, pp. 576-582.

Holl, D. L. (1939), "Shearing Stresses and Surface Deflections due to Trapezoidal Loads," *Proceedings, Highway Research Board*, Vol. 19, pp. 409-423.

Holl, D. L. (1941), "Plane Strain Distribution of Stress in Elastic Media," Iowa Engineering Experiment Station Bull. 148, 55 pp.

Huang, Y. H. (1968), "Stresses and Displacements in Nonlinear Soil Media," *Proceedings ASCE*, Vol. 94, SMl, pp. 1-19.

Jelinek, R. (1948a), "Der Boden als Querisotropes Medium," Abhandlungen uber Bodenmechanik und Brundbau, E. Schmidt, Berlin, pp. 19-24.

Jelinek, R. (1948b), "Die Kraftausbreitung im Verallgemeinerten Ebenen Spannungszustand fur Querisotrope Boden," Abhandlungen uber Bodenmechanik und Grundbau, E. Schmidt, Berlin, pp. 24-27.

Jelinek, R. (1948c), "Die Draftausbreitung im Halbraum fur Querisotrope Boden," Abhandlungen uber Bodenmechanik und Grundbau, E. Schmidt, Berlin, pp. 28-33.

Jones, A. (1962), "Tables of Stresses in Three-Layer Elastic Systems," Highway Research Board Bulletin No. 342, Stress Distribution in Earth Masses, pp. 176-214.

Jumikis, Alfreds R. (1964), *Mechanics of Soils*, D. van Nostrand Co., Inc., New York City, 483 pp.

Jurgenson, Leo (1934), "The Application of Theories of Elasticity and Plasticity to Foundation Problems," Proceedings, Boston Soc. of Civil Engr., Vol. 21, pp. 206-241. also in *Contributions to Soil Mechanics, Boston Soc. of Civil Engrs., 1925-1940*, pp. 148-183.

Jurgenson, Leo (1936), "On the Stability of Foundations of Embankments," *Proc., Intern. Conf. on Soil Mech. and Found. Engr.*, Vol. 2, pp. 194-200, Cambridge.

Kezdi, A. (1957), discussion, *Proc., Fourth Int. Conf. on Soil Mech. and Found. Engr.,* Vol. 3, pp. 158-159.

Koning, H. (1957), "Stress Distribution in a Homogeneous, Anisotropic, Elastic Semi-Infinite Solid," *Proc., Fourth Intern. Conf. on Soil Mech. and Found. Engr.,* Vol.ll, pp. 335-338, London.

Krynine, D. P. (1936), discussion, *Trans.* ASCE, Vol 101, pp. 1085-1092.

Love, A. E. H. (1929), "The Stress Produced in a Semi-Infinite Solid by Pressure on Part of the Boundary," *Philosophical Trans. of the Royal Society,* Series A, Vol. 228, pp. 377-420.

Love, A. E. H. (1944), *A Treatise on the Mathematical Theory of Elasticity*, Dover Publications, New York City, 641 pp.

Marguerre, K. (1931), "Druckverteilung durch eine elastische Schict auf starrer rauher Unterlage," *Ing. Archiv*., Vol. 2, pp. 108-117.

Mehta, M. R. and A. S. Veletsos (1959), "Stresses and Displacements in Layered Systems, " Civil Engr. Studies, Structural Research Series No. 178, Dept. of Civil Engr., Univ. of Illinois, Urbana, 116 pp.

Melan, E. (1919), "Die Druckverteilung durch eine elastische Schicht," No. 7/8, Beton und Eisen, p. 83.

Melan, E. (1932), "Der Spannungzustand der durch eine Einzelkraft im Innern beanspruchten Halfscheibe," *Zeitschrift fur angewandte Mathematik und Mechanik*, Bd. 12, pp. 343-346.

Mindlin, R. D. (1936), "Force at a Point in the Interior of a Semi-Infinite Solid," *Physics*, Vol. 7, pp. 195-202.

Mogami, Takeo (1957), "Numerical Tables for Calculation of Stress Components Induced in a Semi-Infinite Elastic Solid When a Force is Applied at a Point in the Interior of the Body," Kajima Construction Technical Research Institute, Tokyo.

Nadai, A. (1931), *Plasticity*, McGraw-Hill Book Co., NYC.

Newmark, N. M. (1940), "Stress Distribution in Soils," *Proc., Purdue Conf. on Soil Mech. and Its Applications,* pp. 295-303.

Newmark, N. M. (1942), "Influence Charts for Computation of Stresses in Elastic Foundations, " Univ. of Illinois Bulletin, Vol. 40, No. 12, Engineering Experiment Station Bulletin Series 338, 28 pp.

Newmark, N. M. (1947), "Influence Charts for Computation of Vertical Displacements in Elastic Foundations," Univ. of Illinois Bulletin, Vol. 44, No. 45, Engr. Exp. Station Bull. Series No. 367, 14 pp.

Ohde, J. (1939), "Zur Theorie der Druckverteilung im Baugrunde," *Der Bauingenieur*, Vol.

20, pp. 451-459.

Osterberg, J. 0. (1957), "Influence Values for Vertical Stresses in a SemiInfinite Mass Due to an Embankment Loading," *Proc., Fourth Intern. Conf. on Soil Mech. and Found. Engr.*, Vol. 1, pp. 393-394.

Palmer, L. A. (1938), "Principles of Soil Mechanics Involved in the Design of Retaining Walls and Bridge Abutments," *Public Roads*, Vol. 19, pp. 193-207.

Palmer, L. A. (1939), "Stresses Under Circular Loaded Areas," *Proc., Highway Research Board*, Vol. 19, pp. 397-408.

Passer, Walter (1935), "Druckverteilung durch eine elastische Schicht," Akad. der Wissenschaften, Wein, Math.-Natur. Klasse., Sitzungsberichte. Abt. 2a, Vol. 144, pp. 267-275.

Peattie, K. R. (1959), "The Calculation of Stresses and Displacements in Layered Systems," *Proc., Symposium on Vibration Testing of Roads and Runways*, Koninkljke/Shell Laboratory, Amsterdam.

Peattie, K. R. (1962), "Stress and Strain Factors for Three-Layer Elastic Systems," Highway Research Board Bulletin No. 342, *Stress Distribution in Earth Masses*, pp. 215-253.

Peattie, K. R. (1963), "A Fundamental Approach to the Design of Flexible Pavements," *Proc., Intern. Conf. on the Structural Design of Asphalt Pavements*, Univ. of Michigan.

Pickett, G. (1938), "Stress Distribution in a Loaded Soil with Some Rigid Boundaries," *Proc., Highway Research Board*, Vol. 18, Part 2, pp. 35-48.

Pickett, G. and K. Y. Ai (1954), "Stresses in Subgrade Under a Rigid Pavement," *Proc., Highway Research Board*, Vol. 33, pp. 121-129.

Schiffman, R. L. (1957), "The Numerical Solition for Stresses and Displacements in a Three Layer Soil System," *Proc., Fourth Intern. Conf. on Soil Mech. and Found. Engr.,* Vol. 2, pp. 169-173.

Schiffman, R. L. and B. D. Agarwala (1960), "Stresses and Displacements Due to a Rigid Surface Loading on an Elastic Soil Underlain by Rock," Rensselaer Polytechnic Institute, Research Division, Troy, New York.

Schiffman, R. L. and B. D. Aggarwala (1961), "Stresses and Displacements Produced in a Semi-Infinite Elastic Solid by a Rigid Elliptical Footing," *Proc., Fifth Intern. Conf. on Soil Mech. and Found. Engr*., Paris, Vol. 1, pp. 795-802.

Schiffman, Robert L. (1963), Discussion, Highway Research Record, No. 39, pp. 78-81.

Scott, R. F. (1963), *Principles of Soil Mechanics*, Addison-Wesley Publ. Co., Inc. 550 pp.

Sowers, George F. and Aleksandar B. Vesic (1962), "Vertical Stresses in Subgrades Beneath Statically Loaded Flexible Pavements," *Highway Research Board Bulletin 342*, pp. 90-119.

Spangler, M. G. and H. 0. Ustrud (1940), "Wheel Load Stress Distribution Through Flexible Type Pavements," *Highway Research Board Proc*., Vol. 20, pp. 235-257.

Taylor, D. W. (1948), *Fundamentals of Soil Mechanics,* John Wiley and Sons, New York City, 700 pp.

Terzaghi, Karl (1943), *Theoretical Soil Mechanics*, John Wiley and Sons, New York City, 510 pp.

Timoshenko, S. (1948), *Theory of Elasticity*, McGraw-Hill Book Co., New York City, pp. 338-339.

Todhunter, Isaac and Karl Pearson (1886), *A History of the Theory of Elasticity and of the Strength of Materials, From Galilei to the Present Time,* Vol. 1, Galilei to Saint-Venant to Lord Kelvin, Part I, Cambridge University Press, 762 pp.

Todhunter, Isaac and Karl Pearson (1893), *A History of the Theory of Elasticity and of the Strength of Materials, From Galilei to the Present Time,* Vol. II, Saint-Venant to Lord Kelvin, Part II, Cambridge University Press, 546 pp.

Ueshita, K. and George G. Meyerhof (1967), "Deflection of Multilayer Soil Systems," *Proc. ASCE*, Vol. 93, SM5, pp. 257-282.

U.S. Army Waterways Experiment Station (1953), "Investigation of Pressures and Deflections for Flexible Pavements, Report No. 3, Theoretical Stresses Induced by Uniform Circular Loads," Tech. Memorandum No. 3-323, Vicksburg, Miss.

Vesic, A. B. (1963), "The Validity of Layered Solid Theories for Flexible Pavements," *Proc., Intern. Conf. on the Structural Design of Asphalt Pavements,* Univ. of Michigan.

Vogt, Fredrik (1925), "Uber die Berechnung der Fundamentdeformation," Norske Videnskaps-Akademi, Oslo, Avhanklinger, Math.-Natur. Klasse.

Westergaard, H. M. (1938), "A Problem of Elasticity Suggested by a Problem in Soil Mechanics; Soft Material Reinforced by Numerous Strong Horizontal Sheets," Contributions to Mechanics of Solids, Stephen Timoshenko Sixtieth Anniversary Volume, MacMillan Co., NYC, pp. 268-277.

Westmann, R. A. (1963), "Layered Systems Subjected to Surface Shears," *Jour. , Engineering Mechanics Division*, ASCE, Vol. 89, EM6, pp. 177-191.

Wolf, K. (1935), "Ausbreitung der Kraft in der Halbebene und im Halbraum bei Anisotropem Material," Zeitschrift Angew. Math. und Mech., Vol. 15, pp. 249-254.